

Ion-Sensitive

7. Ion-Sensitive Electrodes

Hans-Hermann Rüttinger

Part B | 7.1

In this chapter we introduce the basic methods of electroanalysis that utilize electrochemical reactions at the interface between the solution to be analyzed and different electrodes. Potentiometry, i. e., 7 equilibrium measurements with negligible current is discussed in detail, especially the newer developments of ion-selective electrodes. Experiments that involve charge transfer across the interface are discussed as well, to provide an overview of the most established electroanalytical methods and sensors, comprising constant potential, swept potential, and constant current in quiet solutions or with forced mass transfer.

7.1	Fundamentals of Potentiometry	207
7.1.1	Reference Electrodes	208
7.1.2	Simple Indicator Electrodes.....	210
7.1.3	Membrane Electrodes	210
7.1.4	Characterization of Ion-Selective Electrodes	217
7.1.5	Direct Potentiometric Determination of Concentrations ...	218
7.1.6	Models of ISE Response	218
7.1.7	All Solid-State Electrodes.....	222
7.1.8	Ion-Selective Field Effect Transistor (ISFET)	225
7.1.9	Drug Sensitive Electrodes	226
7.2	Application of ISE	226
7.2.1	Gas-Sensitive Electrodes and Biosensors	226
7.2.2	Detectors in Flow Systems.....	227
7.3	Amperometric and Voltammetric Methods	227
7.3.1	Experimental Methods	227
7.3.2	Electrochemical Reaction Mechanisms	233
	References	237

The goal of electroanalysis is to gain chemical information about a sample such as the constituents, its concentration and distribution, and even reactions and state of equilibria directly from electrical measurable readings. Electrical data such as voltage and current are easy to measure and in modern apparatus they may be fed into a powerful microcontroller to calculate the final results. The fundamentals of electroanalysis are more than a hundred years old, but the development still goes on, especially in the field of nanoscaled sensors and their combinations with specific biochemical reactions as immunoassays or enzymatic catalysis.

7.1 Fundamentals of Potentiometry

Let us consider a simple measurement of a voltage. What is the interface between the instrument and the chemistry in a beaker? In Fig. 7.1 a principal experimental setup is shown.

Both plug-ins of the instrument are connected through a copper wire to a piece of copper or silver,

Ion-selective electrodes (ISE) are an important subgroup of electrochemical sensors. They are small in size, even downscaled to the micrometer range, and easy to interface with low-power consuming inexpensive instruments. They are now commercially available for the determination of a large number of inorganic and organic ions, which are very attractive features concerning practical applications. A huge number of scientific works have been done in the last century and the rate of publication increased steadily up to 1978; since then a constant output of about 400 papers per year has been published [7.1].

each immersed in a diluted solution of its salts, here copper sulfate and silver sulfate.

A voltage of +0.412 V is measured as the potential difference of the two half cells. Note that the positive plug-in of the instrument is connected to the silver metal, the right electrode; and the common plug-in to

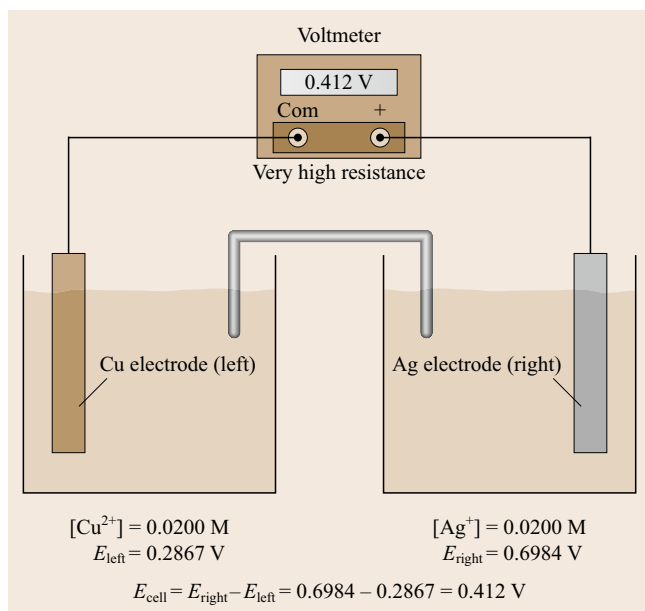
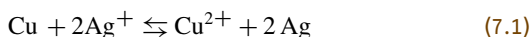


Fig. 7.1 Measurement of the potential between two half cells (after [7.2])

the copper, the left electrode. The observed voltage corresponds to the free enthalpy of the reaction



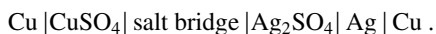
that would proceed to the equilibrium from left to right. The oxidation of the copper anode and the reduction of the silver cation are separated in space and the charge must be transported through the conductors to make the reaction go. The molar free enthalpy of the reaction equals the electrical energy of the reversible and isothermal charge transfer and is given by the product of voltage and charge

$$\Delta G^0 = -zFE = -RT \ln K_{\text{eq}}. \quad (7.2)$$

By replacing the voltmeter with a resistor, the reaction runs to the right side with a rate of reaction proportional to the electric current, and the setup works as a galvanic element delivering electricity at the cost of the chemical system. The sign of the enthalpy is therefore negative by convention.

The voltage measured by the instrument is the sum of all the differences of potentials that arise at any phase boundary in the electric circuit.

The setup in Fig. 7.1 is therefore symbolized by the scheme



The potential differences at the interface between different metals are small and are mutually compen-

sated, but the transition from metal with electrons as charge carriers to an electrolyte with ions as charge carriers and vice versa involve redox reactions. The free energy of those reactions is related to the potential difference at their interfaces.

In the case of the right half cell



δG corresponds to the difference of the chemical potentials of pure silver and the silver ion in the solution

$$\delta G = -zFE = \mu_{\text{Ag}} - \mu_{\text{Ag}^+} = \mu_{\text{Ag}}^\ominus - [\mu_{\text{Ag}^+}^\ominus + RT \ln(a_{\text{Ag}^+})] \text{ with } z = 1, \quad (7.4)$$

$$E = \frac{\mu_{\text{Ag}^+}^\ominus - \mu_{\text{Ag}}^\ominus}{zF} + \frac{RT}{zF} \ln(a_{\text{Ag}^+}). \quad (7.5)$$

The constant part will be summarized in the standard potential

$$E = E^0 + \frac{RT}{zF} \ln(a_{\text{Ag}^+}). \quad (7.6)$$

This is the well-known Nernst equation. The general form is

$$E = E^0 + \frac{RT}{zF} \ln \frac{a_{\text{ox}}}{a_{\text{red}}}. \quad (7.7)$$

The potential of a half cell can't be measured, because you can't connect the electrolyte to the input of an instrument without establishing a second electrode. A complete cell is needed, and to get thermodynamically defined potential differences between the two electrodes any external charge transfer must be prevented in order to measure a non-disturbed equilibrium potential difference. That means open circuit conditions with a high impedance instrument. Commercial instruments for potentiometric measurements have an input resistance better than $1 \times 10^{12} \Omega$. Nevertheless a small charge transfer to achieve the equilibrium must occur to charge the double layer at the electrode and to charge the capacitance of the cables and the input stage of the instrument.

7.1.1 Reference Electrodes

As the Nernst equation implies, direct analytical information can be drawn from potentiometric measurements. For such purposes the second electrode of the cell should remain at a constant and reproducible potential, independent of the analytical matrix. Only then does it work as a proper reference electrode.

A very reproducible half cell is the standard hydrogen electrode, to which all electrode potentials are referenced to by convention.

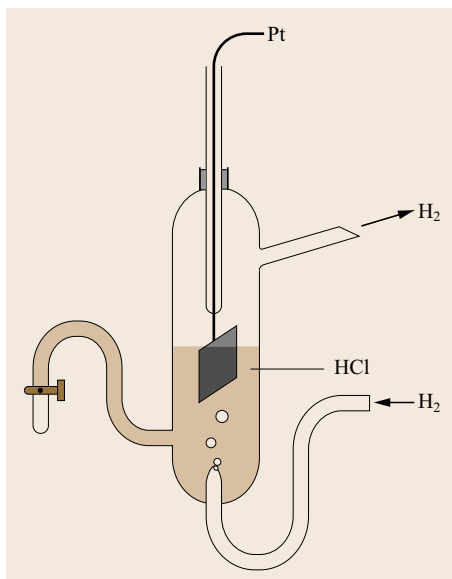


Fig. 7.2 Standard hydrogen electrode. The pressure of hydrogen is 1 bar, the activity of the hydrochloric acid 1N

The standard hydrogen electrode is based on the redox equilibrium between molecular hydrogen and hydronium ions



$$E = E_{\text{H}_2}^0 + \frac{RT}{2F} \ln \frac{a_{\text{H}^{+}}^2}{p_{\text{H}_2}}. \quad (7.9)$$

This reaction is catalyzed on the surface of a rough platinum electrode and the electrons are transferred from

the adsorbed hydrogen to the metal. The potential of the hydrogen electrode with $a_{\text{H}^{+}} = 1$ and a hydrogen pressure of 1 bar is defined as $E_{\text{H}_2} = 0\text{V}$.

Figure 7.2 shows a possible construction of a standard hydrogen electrode.

For practical use the standard hydrogen electrode is cumbersome and can be replaced in the lab by more convenient electrodes. The majority of these reference electrodes are metal electrodes in solution saturated with a low soluble salt of the same metal and an excess of its corresponding anion. These *second type* electrodes exhibit a constant potential against the standard hydrogen electrode and are insensitive against polarization by small currents.

A typical construction of the widely used silver/silver chloride electrode is shown in Fig. 7.3.

The potential of this electrode depends on the concentration of chloride, because the solubility product of the silver chloride determines the activity of the silver ions (Table 7.1). Thus, two equilibria are involved in the potential determination process

$$L = a_{\text{Ag}^{+}} a_{\text{Cl}^{-}}, \quad (7.10)$$

$$E = E^0 + \frac{RT}{F} \ln \frac{L}{a_{\text{Cl}^{-}}}, \quad (7.11)$$

$$E = E^0 + \frac{RT}{F} \ln L - \frac{RT}{F} \ln a_{\text{Cl}^{-}}. \quad (7.12)$$

To prevent contamination of the inner solution an additional salt bridge with a second junction is added in the advanced construction (Fig. 7.3b). Both solutions are separately exchangeable.

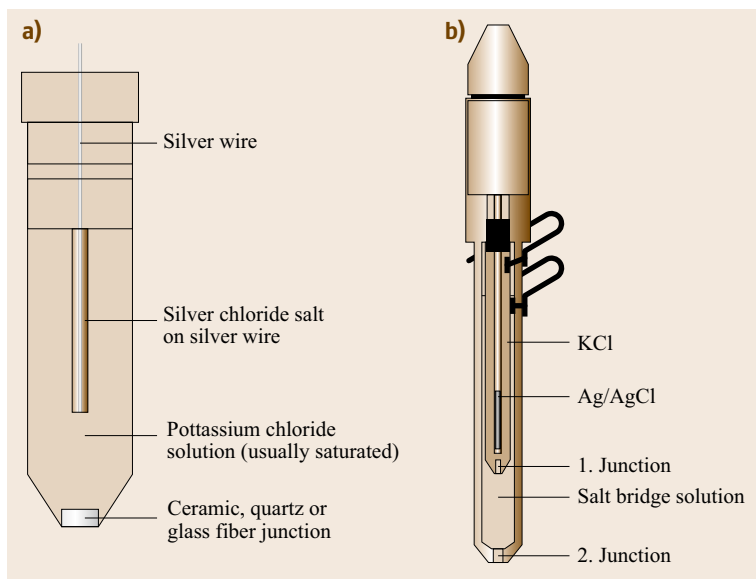


Fig. 7.3a,b Silver/silver chloride electrode. (a) Simple reference electrode. (b) Double junction reference; the salt bridge solution will be adapted to the analytical problem

Table 7.1 Examples of silver/silver chloride electrodes

Electrolyte	Potential against standard hydrogen electrode (V)	Temperature coefficient at 25 °C (mV/K)
Sat. KCl	+0.197	-1.01
3.5 M KCl	+0.205	-0.73
3.0 M KCl	+0.210	
1.0 M KCl	+0.235	+0.25
0.6 M KCl	+0.250	
Seawater	+0.266	

Table 7.2 Some reference electrodes

Electrode	Potential against standard hydrogen electrode (mV)
Hg/Hg ₂ Cl ₂	+245.0
Hg/Hg ₂ Br ₂	+139.56
Ag/AgBr	+71.31
Pb/PbSO ₄	-276.0
Ag/AgJ	-152.25

The salt bridge is filled with potassium chloride or nitrate to minimize an additional potential difference at the junction of the salt bridge and the analyte solution. The diffusion coefficients of potassium ions and chloride are nearly the same, thus a minimal diffusion potential is produced.

Other reference electrodes are listed in Table 7.2.

7.1.2 Simple Indicator Electrodes

Whereas the potential of the reference electrode is independent of the analyte, the potential of the indicator electrode should be reliable and be a specific function of the interesting constituent in the solution.

Metal Electrodes

As already shown, the potential of a metal electrode is directly related to the activity of its corresponding ions. The usage of this kind of electrodes is limited because the underlying redox reaction is disturbed if other interfering redox systems are present in the analytical matrix.

Nevertheless, a simple silver wire serves as an indicator in argentometric titrations and since the activity of copper ions is strongly shifted by complexation, a copper wire can be used as indicator for complexometric titrations. It only needs the addition of a small amount of copper ethylenediaminetetraacetate (EDTA)-complex to the solution.

The activity of bismuth ions at the surface of a bismuth electrode is related to the solubility product of the bismuth hydroxide and the hydroxyl ions. In absence

of strong oxidizing or reducing agents this electrode is used as a simple and rough pH-electrode. An antimony electrode works analogously.

Inert Electrodes

Noble metal electrodes as well as carbon electrodes are not directly involved in the redox process, but are able to exchange electrons with the redox systems in the surrounding solution. That way the redox potential of a solution is measured and the ratio of $a_{\text{ox}}/a_{\text{red}}$ of a corresponding redox couple according to the Nernst equation is achieved.

These electrodes are very useful for the registration of redox titrations. The endpoint is indicated as the steepest change of the potential. Contrary to redox titration, the reliability of direct redox potential measurements is often hampered as the electron transition at the electrode is kinetically hindered in many cases, especially in biological systems where redox active macromolecules cannot exchange electrons, because the distance of their redox centers is too far from the surface of the electrode.

7.1.3 Membrane Electrodes

A schematic setup is given in Fig. 7.4. Test solution and reference solution are separated by a permselective membrane and the potential difference is measured by two reference electrodes. Alternatively the inner reference electrode is replaced by a direct metallic contact. As already shown, the transfer of any charge carrier across the border of two separated phases causes a potential difference at the border. If not disturbed, the systems run to an equilibrium where the electrical potential compensates the differences in the chemical potentials of the two phases. Provided the charge transfer is limited to only one ion species, the activity ratio of that ion species is related to the electrical potential between the two phases

$$E = E_{\text{ass}} + \frac{RT}{zF} \ln \frac{a_{\text{I}}}{a_{\text{II}}} \quad (7.13)$$

In the case of cations z is positive and in the case of anions z is negative. At room temperature (25 °C) the factor RT/F together with a change from the natural to the common decadic logarithm results in a factor of 59 mV. Thus, a tenfold change of activity results in a potential shift of 59 mV in the case of $z = 1$ or 29 mV for $z = 2$. If the two reference electrodes exhibit identical behavior and the membrane is symmetric, then E_{ass} vanishes.

The permeation selectivity of the membrane is crucial for the performance of these ion-selective electrodes.

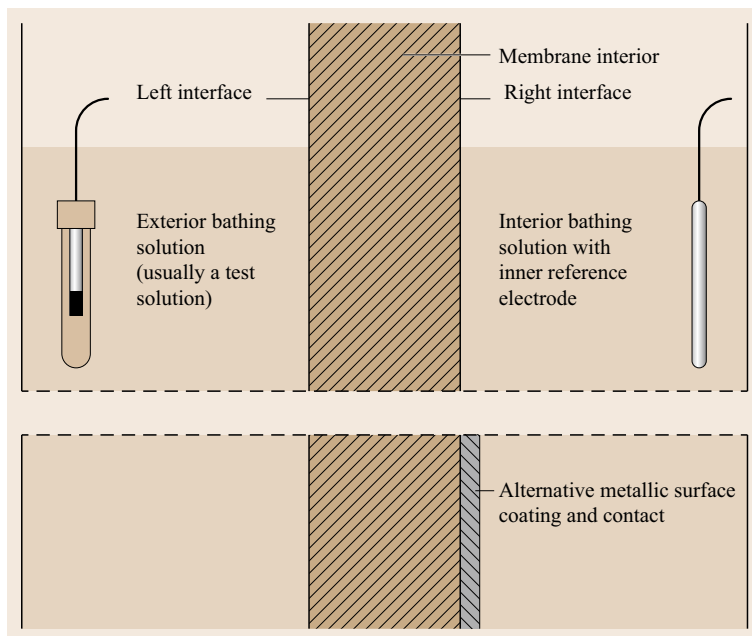


Fig. 7.4 Membrane electrode (after [7.3])

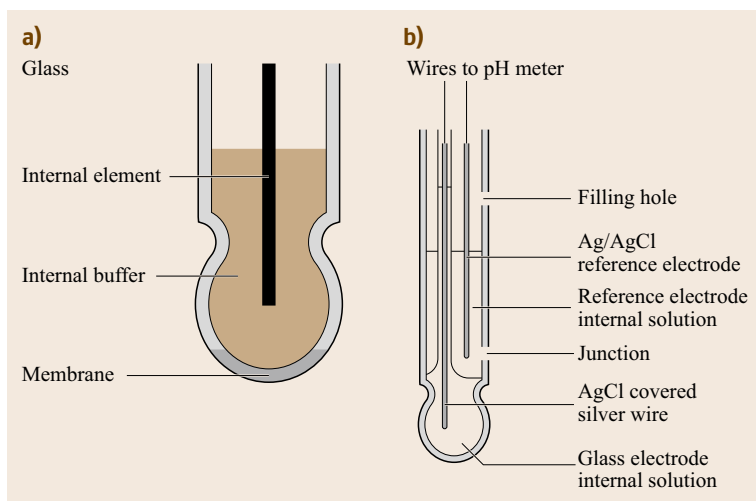


Fig. 7.5 (a) A single glass electrode. (b) Combined with a silver/silver chloride reference electrode to a one-rod pH sensor

The Glass Electrode

The best selectivity so far is achieved with the H^+ selective glass membranes; nearly all pH measurements are done with this electrode. Since the glass doesn't transport electrons it is insensitive towards oxidizing or reducing agents. The glass electrode is more than hundred years old and a lot of research has been done to gain a closer insight into the potential-forming mechanism as well as to construct robust electrodes for applications in very different media. Often the glass electrode is completed with a reference electrode to unit in one rod.

A typical construction of a glass electrode is shown in Fig. 7.5.

The best-known glass for pH electrodes is Corning 015 composed of about Na_2O 22%, CaO 6%, SiO_2 72%. In contact with water, the surface layer is hydrated and parts of the sodium ions are exchanged by protons. This gel layer, extending 1–100 nm into the membrane, is responsible for the electrochemical behavior of the electrode.

At high pH values, that means at low hydronium concentrations and high concentrations of univalent cations the glass electrode is even sensitive to sil-

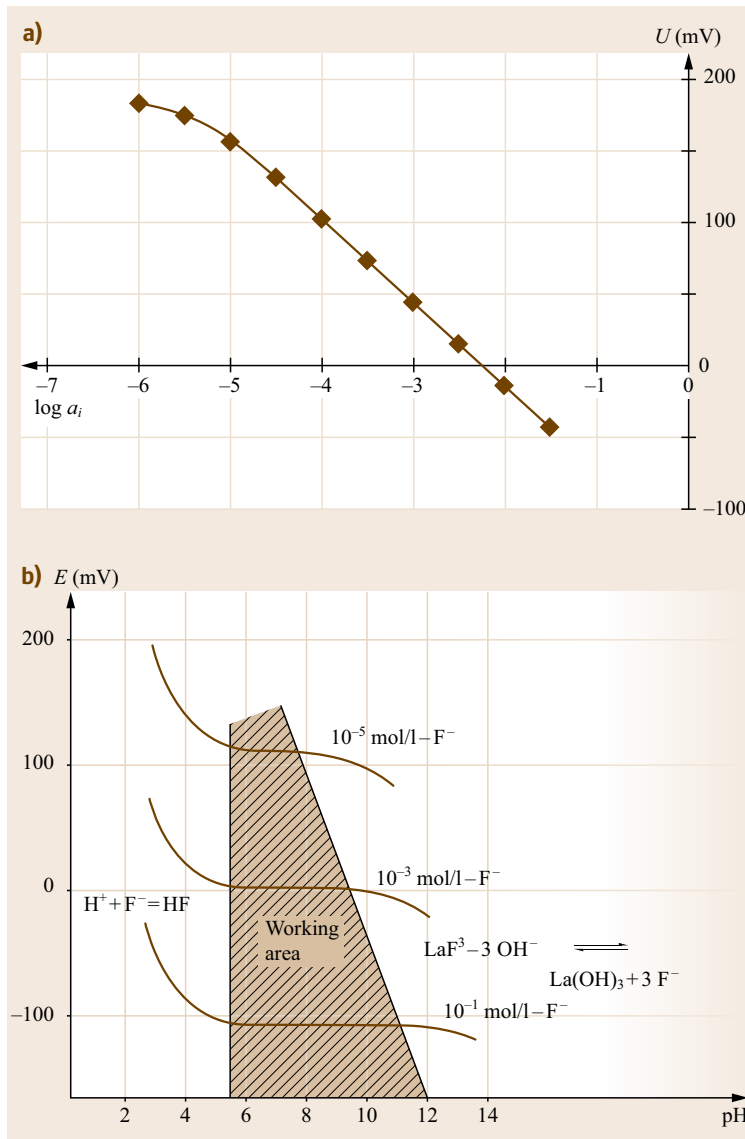
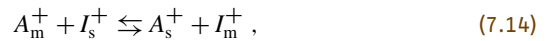


Fig. 7.6a,b Fluoride sensitive electrode. (a) Response function. (b) Influence of different pH on the working area (after [7.4])

ver, potassium or sodium ions. The sensitivity against sodium ions results in an alkali error in pH measurements. It was found that a part replacement of the sodium component in the glass by lithium diminishes the cross sensitivity towards sodium ions.

On the other side the modification of the glass composition by addition of a certain quantity of alumina results in a sodium-selective electrode. Considering the ion-selective membrane as a selective ion exchanger, the effects of interfering ions can be expressed by the exchange equilibrium between the analyte ion (A_m) at the surface of the membrane and the interfering ion (I_s) from the solution (Sect. 7.1.4)



$$K_{m-s} = \frac{a_{A_s^+} a_{I_m^+}}{a_{A_m^+} a_{I_s^+}} . \quad (7.15)$$

The cross sensitivity of an electrode based on this equilibrium is described by an extension of the Nernst equation introduced by *Nikolsky* and *Eisenmann* [7.5]

$$E = E_{\text{ass}} + \frac{RT}{zF} \ln \left[a_A + \sum_{a_1} K_{A-1} (a_1)^{z_A/z_1} \right] . \quad (7.16)$$

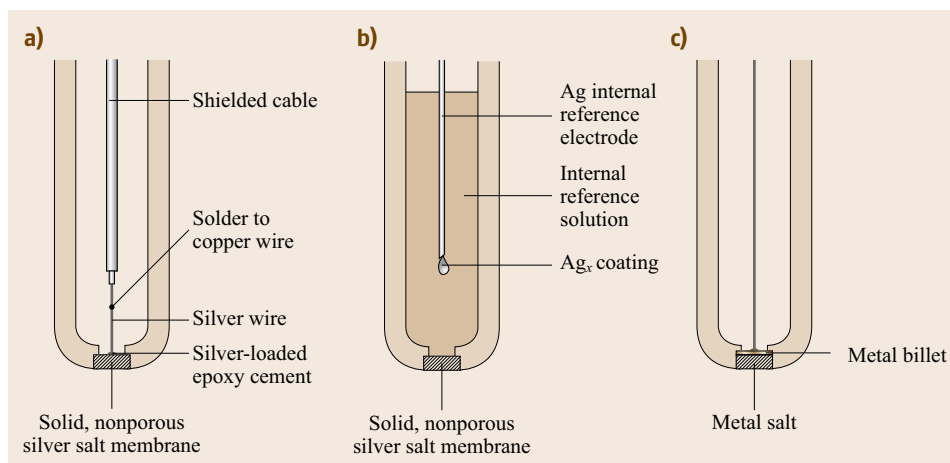


Fig. 7.7a–c Constructions of crystalline membrane electrodes (a) All solid state electrode, (b) electrode with internal reference solution, (c) electrode of the second kind (after [7.3])

This equation is applicable to all ion-selective electrodes.

Crystalline Membrane Electrodes

The membrane of this type of electrodes consists of a single or polycrystalline ion-conducting membrane.

Fluoride Sensitive Electrode

A membrane from a lanthanum fluoride single crystal, doped with EuF_2 , transports fluoride ions very selectively. The Eu^{2+} creates lattice vacancies along which the fluoride ions move. Even with a thousand-fold excess of other halide ions and nitrate, phosphate or hydrogen carbonate do not interfere and the electrode shows a Nernstian behavior from concentration ranges $1-1 \times 10^{-6} \text{ mol l}^{-1}$. In very alkaline solutions the formation of a lanthanum hydroxide layer at the surface of the electrode interferes at low F^- concentrations, and in acidic solutions the fluoride ion associates with the proton, but only the free fluoride ion is measured by the electrode. These two effects define the working area of the electrode as illustrated in Fig. 7.6b. As fluoride forms strong complexes with aluminum and ferric ions these ions interfere and must be masked. If true concentrations and not activities are desired as a result, then the electrode must be calibrated and used in solutions of the same ion strength to hold the activity coefficient constant. This is generally realized as in most direct potentiometric determinations by the addition of a total ion strength buffer; it even adjusts the pH to the working range of the electrode.

Silver Sulfide Electrodes

Silver halides and especially silver sulfide exhibit a certain electric conductivity in the solid state. This conductivity is mainly caused by the mobility of the silver ions in this material. Silver sulfide has a very small

conductivity for electrons causing a small influence on oxidizing agents. A variety of electrodes are produced on a base of silver sulfide. Selectivity against halides and pseudo halides is achieved by mixing the corresponding silver halides with the basic silver sulfide. The selectivity coefficients of the different halides relate to the solubility product ratio of the incorporated silver salts. Response against other cations such as lead, copper and cadmium is gained by mixing its sulfides to the silver sulfide. The membranes are produced by pressing the powder of the raw material into a tablet or melting it together. This relatively simple procedure results in polycrystalline membranes. Better sensitivity at low concentrations is claimed with a single crystal membrane, due to the lower solubility of the bigger crystals. A typical construction of a solid membrane electrode is shown in Fig. 7.7. The membrane is tightly glued to a plastic (PVC – polyvinyl chloride) tube and the upper part is filled with the reference electrolyte and equipped with a reference electrode. The liquid reference electrolyte in the electrode is regarded as a weak point in the construction of the electrode and there are several attempts to replace it with a solid construction: solidification of the electrolyte by gelling additives, direct contact of the metal, and welded or glued to the membrane. The potential at the direct interface between membrane and metal, the transition from ionic to electronic conductivity, is not well defined and often causes slow drifting of the overall potential. Recently [7.6] these disadvantages have been overcome and very stable all solid-state ion-selective electrodes can now be constructed (Sect. 7.1.6). Table 7.3 shows a collection of some commercial crystal membrane electrodes.

Liquid Membrane Electrodes

These electrodes gain their analytical information from the potential difference at the interface of two immisci-

Table 7.3 A collection of some commercial crystal membrane electrodes

Electrode	Active membrane	Range (mol/l)	Selectivity log[K]	Recommended pH-range
Ag ⁺	Ag ₂ S	1–1 × 10 ⁻⁷	Cu ²⁺ : -6 Pb ²⁺ : -6	2–9
Cu ²⁺	CuS/Ag ₂ S	0.1–1 × 10 ⁻⁸	Ag ⁺ , Hg ²⁺ must be absent	0–14
Cu ²⁺	CuSe single crystal	1–1 × 10 ⁻⁶	Pb ²⁺ : -3 Cd ²⁺ : -5 Ag ⁺ : 6 Hg ²⁺ : 4	0–14
Cd ²⁺	CdS/Ag ₂ S	0.1–1 × 10 ⁻⁷	Ag ⁺ , Hg ²⁺ must be absent Fe ²⁺ : 2.3 Pb ²⁺ : -0.3 Zn ²⁺ : -1	1–14
Pb ²⁺	PbS/Ag ₂ S	0.1–1 × 10 ⁻⁶	Ag ⁺ , Hg ²⁺ , Cu ²⁺ must be absent Zn ²⁺ : -3.5 Fe ³⁺ : 0 Cd ²⁺ : 0	2–14
S ²⁻	Ag ₂ S	1–1 × 10 ⁻⁶	Traces of Hg ²⁺ interfere, proteins must be absent Cl ⁻ : -15 J ⁻ : -9 CN ⁻ : -2	13–14
Cl ⁻	AgCl/Ag ₂ S	1–1 × 10 ⁻⁷	Br ⁻ : 2 J ⁻ : 3	1–5
F ⁻	LaF ₃ single crystal	1–1 × 10 ⁻⁶	Cl ⁻ : -4 Br ⁻ : -4 NO ₃ ⁻ , SO ₄ ²⁻ : < -3	4–8

ble liquid phases, the aqueous sample and the organic membrane phase. The liquid organic phase is often fixed in the pores of a hydrophobic porous membrane. Some constructions of such electrode are shown in Fig. 7.8. For better handling the liquid membrane may be solidified by the addition of polymers with no change of the working principle.

Liquid Ion Exchangers

Glass electrodes and the silver sulfide electrodes may be regarded as ion exchangers with fixed ions. On this basis several organic and inorganic solid ion exchangers have been tested as materials for ion-selective electrodes. These tests failed because the mobility of the probed ion is drastically reduced when bound to a fixed

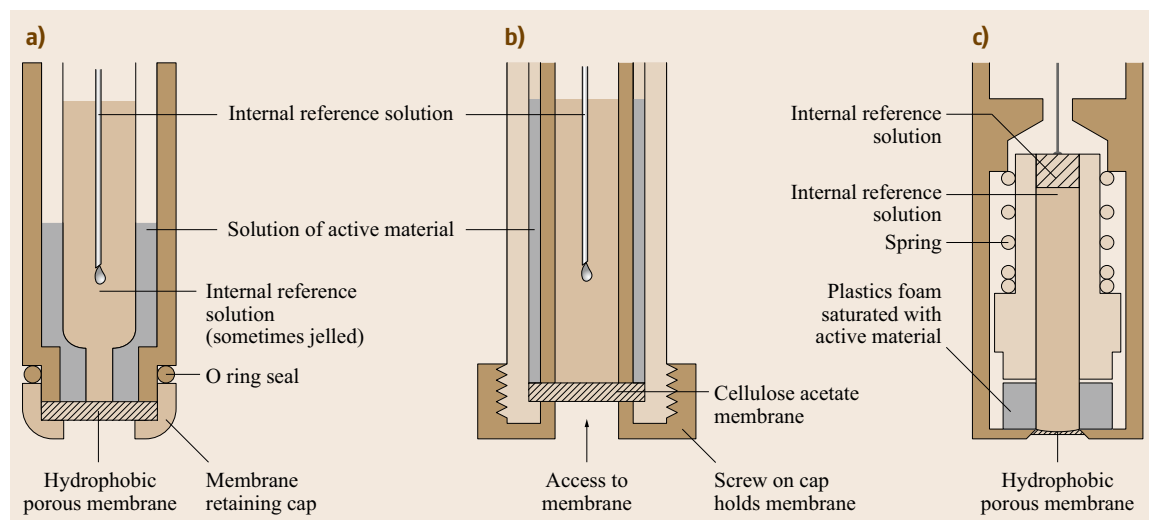
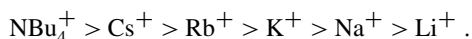


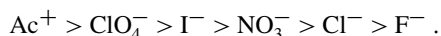
Fig. 7.8a–c Constructions of liquid membrane electrodes (a,b) allow easy replacement of the membranes and (c) contains a reservoir of the active material in a foam (after [7.3])

charge in the ion exchanger. In the liquid phase the complex between the measured ion and the dissolved ion exchanger is mobile. The specific ion exchanger is dissolved in a polar, but not water miscible, organic solvent and the specific charge transfer from the aqueous to the organic phase governs the potential difference at the interface. For stability of the electrode the boiling point of the organic phase should be high to avoid evaporation. The affinity of the ion exchanger to the analyte ion should be high and the ion pair very hydrophobic and nonsoluble in water. The organic phase contains the ion exchanger with the analyte as a counter ion. As solvents, long chain alcohols are used, or nitrobenzene or nitrophenylethers. If the interaction between the liquid ion-exchanger and the analyte ion only consists of electrostatic attraction of the oppositely charged sites, then the selectivity between different sensed ions is dictated mainly by the extraction behavior of the solvating membrane medium. The ionic extraction constants are comparatively small for ions that are strongly hydrated in the aqueous phase and large for lipophilic organic ions.

Therefore the following sequence (Hofmeister row) is obtained for membrane electrodes based on cation exchangers, e.g., tetraphenylborate in nitroaromatic solvents



An analogous sequence is obtained for anion exchangers (e.g., quarternary ammonium salts)



A liquid membrane needs a special construction of the electrode to hold the liquid in place.

Therefore their use is limited to special applications such as microelectrodes for intracellular measurements, and most commercial electrodes use solidified liquid membranes working on the same theoretical background.

Tiny glass capillaries with an inner diameter lower than a micrometer are used for monitoring of ion activities in living cells. The ion-selective liquid is placed at the tip and fixed by the capillary adhesion (Fig. 7.9).

Solidification is achieved by addition of polymers such as PVC, polyacrylates or silicon rubber to the liquid. The construction of solidified membrane electrodes is quite simple as shown in Fig. 7.10.

The inner solution with the reference electrode is partly solidified by the addition of a hydrogel like poly(hydroxyl ethyl acrylate). The simplest con-

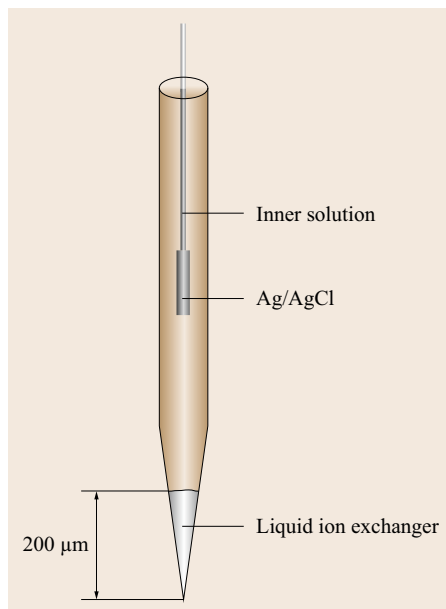


Fig. 7.9 Ion-selective microelectrode with liquid ion exchanger

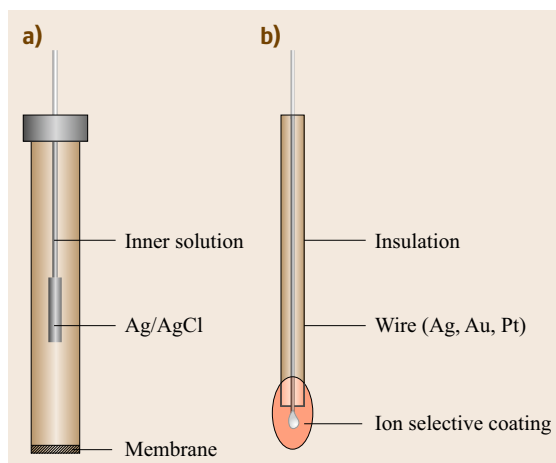


Fig. 7.10a,b Ion-selective polymer membrane electrode. (a) With inner reference. (b) Coated wire electrode

structions are the *coated wire electrodes*. They are easy to prepare by dipping a gold, silver or platinum wire into a solution of the ion selective cocktail and isolate the rest of the metal. Unfortunately these electrodes are suffering from drift and other instabilities, because the transition of charge from the membrane to the metal is not really defined. Newer developments successfully overcame these shortcomings and now some all-solid-state electrodes with superior stability and sensitivity are available. The principle of these electrodes will be discussed in Sect. 7.1.6.

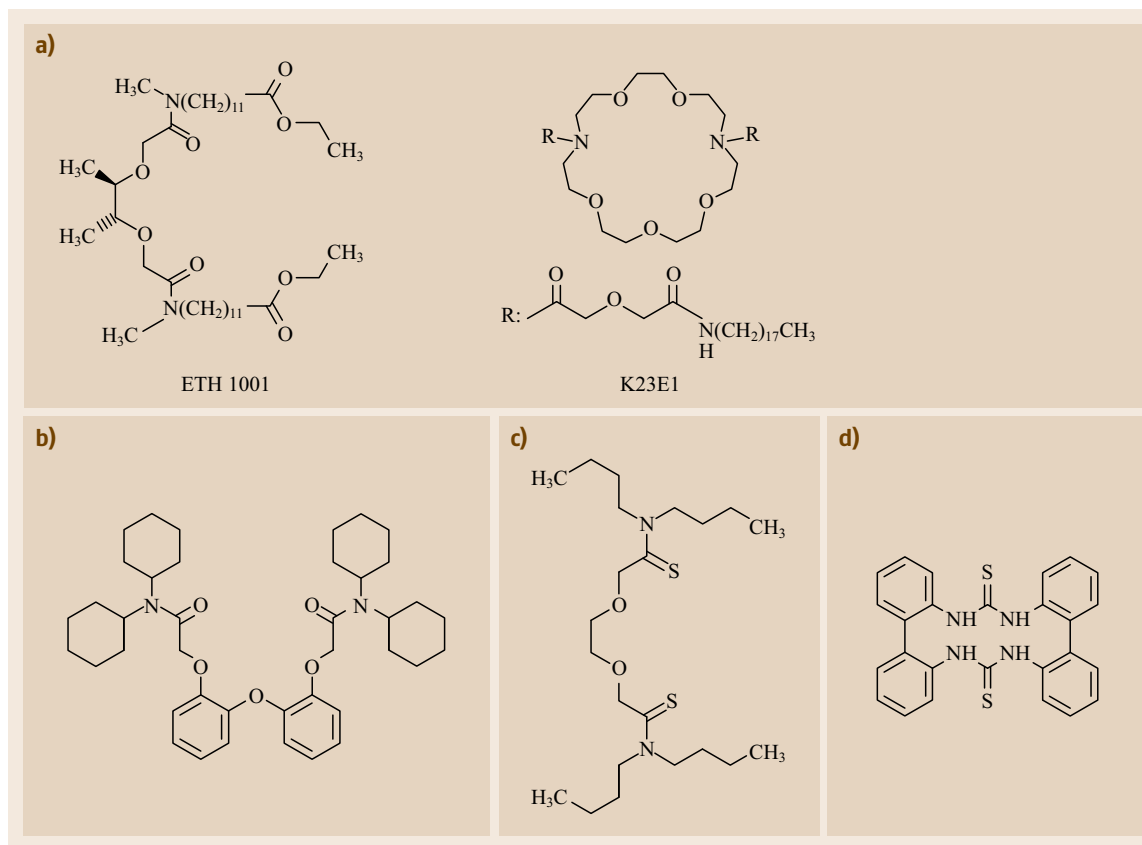


Fig. 7.12a–d Ion carriers for earth alkali cations and nitrate (a) Ca²⁺, (b) Ba²⁺, (c) Cd²⁺, (d) NO₃⁻

As counteraction for the nitrate electrode a small amount of tridodecylammonium (nitrate) is added. A brief selection of liquid membrane electrodes with the used ion carriers is given in Table 7.4.

7.1.4 Characterization of Ion-Selective Electrodes

As already pointed out, the equilibrium potential difference between both sides of an ion-selective membrane strictly corresponds to the difference in the thermodynamically defined chemical potentials on these sides.

This behavior is expressed by the Nernst equation and does not depend on a special structure of the ideal ion-selective membrane.

In practice, however, deviation from this ideal behavior is experienced and a huge amount of research has been undertaken to find out the reasons for this nonideal behavior.

Different levels of theory have been developed for the qualitative and quantitative description of the effects, and resulting theoretical understandings of

the potential forming processes at and in the membranes have even resulted in improved sensors and in the last decade to a *new wave of ion-selective electrodes* [7.9].

Potentiometric Response

The most important information for the user of ISEs is the selectivity and the lower limit of detection. Fig. 7.13 shows a typical calibration curve for a univalent cation. Due to leaching of the main ion from the membrane and the influence of interfering ions in the matrix, the electrode becomes more and more insensitive at low concentrations and finally the calibration curve becomes parallel to the activity axis. The detection limit is the intercept of the Nernstian part and the constant part of the calibration curve.

Selectivity Coefficients

The selectivity coefficient can be calculated from the difference between the calibrating curve of the main ion and the interfering ion. Two possible methods of evaluation can be derived based on the Nikolsky equation.

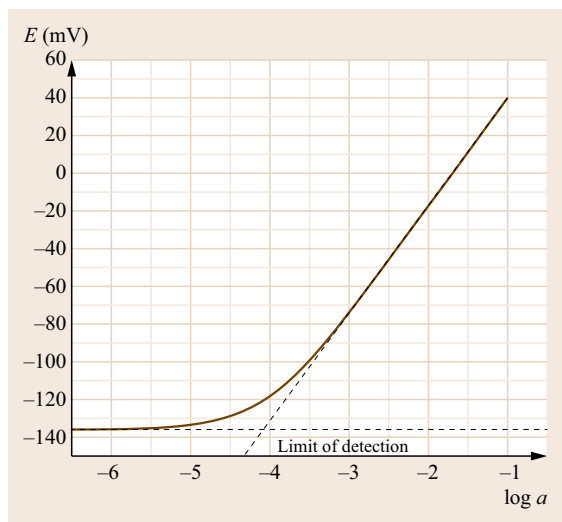


Fig. 7.13 Response function and detection limit of an ion-selective electrode, according to the Nikolsky–Eisenman equation

From the potential difference at the same concentration (I in Fig. 7.14)

$$\log(K_{i,j}) = \frac{E_2 - E_1}{S}, \quad (7.17)$$

or the ratio of the activities at the same potential (II in Fig. 7.14)

$$\log(K_{i,j}) = \frac{a_i}{a_j}. \quad (7.18)$$

It is evident that the selectivity coefficient depends on the concentration, because the deviation from Nernstian response of an electrode in a solution of the pure main ion is usually not included in the Nikolsky equation. More realistic data are obtained from calibration curves of the main ion in the presence of constant concentrations of the interfering ions.

After a sudden change of concentration the potential response needs some time to attain the equilibrium value. The response time during which 90% of the final value is reached depends on the concentration and is about five times longer at a transition from concentrated solutions to diluted than vice versa. To establish a new equilibrium at the surface of the ISE, ions must be transported from and to the surface. This process is facilitated by stirring the bathing solution.

7.1.5 Direct Potentiometric Determination of Concentrations

According to the Nernst equation the potential of an indicator electrode is related to the activity of the mea-

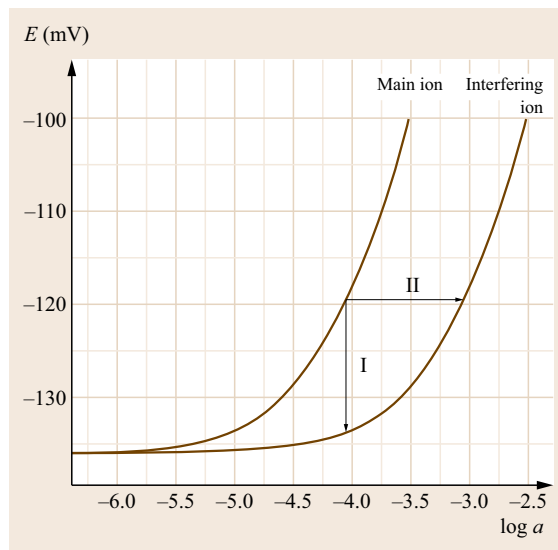


Fig. 7.14 Determination of selectivity coefficients

sured ion in the surrounding solution. This may be a great advantage as very often e.g., in physiology or reaction kinetics and equilibria the field is governed by activities rather than real concentrations. If the concentration data are wanted, then the activity coefficients of the calibration solution and the analytical matrix must be the same. This can be achieved by adjusting the ion strength of sample and standard solutions by the addition of a so-called total ion strength adjustment buffer (TISAB). The additives of this buffer have to be adapted to the analytical problem. In particular, the ions in the buffer should not interfere with the indicator electrode. Not only the ion strength, but the pH is also adjusted by the TISAB to assure a proper working range.

Some examples of ion strength buffers are listed in Table 7.5.

There is no need for ion strength adjustment if calibration and analytical measurement is done in the same matrix. Standard addition is a suitable method to avoid extensive matrix modification and sample preparation.

The addition of inert salts, however, increases the conductivity of the sample, resulting in a short cut of environmental electrical noise and prevents electrokinetic disturbances, caused in streaming media by charge separation at the walls of vessels or tubes.

7.1.6 Models of ISE Response

As the analytical signal is produced at the phase boundary, every change in the bulk analyte composition initiates transport of ions and charge to and from the boundary to establish a new equilibrium. Therefore the potentiometric response is a complex phenomenon that

Table 7.5 Total ion strength adjustment buffer (TISAB) (after [7.10])

Measuring ion	TISAB	For 100 ml solution
Ag ⁺	c(KNO ₃)= 1 mol l ⁻¹	10.110 g
BF ₄ ⁻	c[(NH ₄) ₂ SO ₄]= 2 mol l ⁻¹	26.427 g
Br ⁻	c(KNO ₃)= 1 mol l ⁻¹ or c(NaNO ₃)= 2 mol l ⁻¹	10.110 g 16.999 g
Ca ²⁺	c(KCl)= 1 mol l ⁻¹	7.455 g
Cd ²⁺	c(KNO ₃)= 1 mol l ⁻¹	10.110 g
Cl ⁻	c(KNO ₃)= 1 mol l ⁻¹ or KNO ₃ , Ammonium acetate, Glacial acetic acid or c(NaNO ₃)= 2 mol l ⁻¹	10.110 g 5.06 g 3.85 g 2.8 ml 16.999 g
CN ⁻	c(NaOH) = 0.1 mol l ⁻¹	0.400 g
Cu ²⁺	c(KNO ₃)= 1 mol l ⁻¹	10.110 g
F ⁻	NaCl Glacial acetic acid Trans-1,2-Diamino-cyclohexane-N,N,N,N-tetraacetic acid monohydrate (CDTA, Komplexon IV)	5.84 g 5.75 ml 0.45 g
I ⁻	c(KNO ₃)= 1 mol l ⁻¹ or c(NaNO ₃)= 2 mol l ⁻¹	10.110 g 16.999 g
K ⁺	c(NaCl) = 1–0.1 mol l ⁻¹	5.844–0.584 g
Na ⁺ (glass)	Trishydroxymethyl aminomethane c[(HOH ₂) ₃ CNHN ₂] = 1 mol l ⁻¹ or triethanolamine	12.114 g 7.5 ml
Na ⁺ (plastic)	c(CaCl ₂) = 1 mol l ⁻¹	14.702 g CaCl ₂ 2H ₂ O
NO ₃ ⁻	c[(NH ₄) ₂ SO ₄] = 1 mol l ⁻¹ or c[Al ₂ (SO ₄) ₃] = 0.1 mol l ⁻¹	13.213 g 3.421 g
Pb ²⁺	c(NaClO ₄ H ₂ O) = 1 mol l ⁻¹	14.046 g
S ²⁻	c(NaOH) = 2 mol l ⁻¹	7.999 g
SCN ⁻	c(KNO ₃) = 1 mol l ⁻¹ or acetate buffer pH = 6, c(CH ₃ COO ⁻) _{tot} = 1 mol l ⁻¹	10.110 g

depends on time, the electroactive material and the bathing solution (the analyte) as well as the membrane–solution interface, and their composition and thermodynamic and kinetic properties. The classical total equilibrium models neglect the kinetic effects and assume the membrane potential as a sum of the phase boundary potential and the diffusion potential in the membrane.

In the simple phase boundary model some idealizing assumptions are used:

- No migration effects in the membrane, resulting in zero diffusion potential
- Electroneutrality in the membrane, except the boundary
- Electrochemical equilibrium at the sample–membrane interface
- Solution and membrane phases are ideally immiscible
- No flux of solvent through the membrane.

The phase boundary potential is then

$$E_{\text{PB}} = \frac{RT}{z_i F} \ln k_i + \frac{RT}{z_i F} \ln \frac{a_i}{\bar{a}_i}, \quad (7.19)$$

with a_i the activity of the main ion in the solution and \bar{a}_i the activity of the main ion in the membrane; k_i is an ion partition constant between solution and membrane.

Introducing the exchange equilibrium constant between the main ion i and the interfering ion j at the

membrane surface

$$K_{i,j} = \frac{k_j}{k_i} = \frac{a_i \bar{a}_j}{a_j \bar{a}_i}. \quad (7.20)$$

Simple calculation results in an expression like the Nikolsky equation

$$\frac{a_i}{\bar{a}_i} = \frac{a_i(\bar{a}_i + \bar{a}_j)}{\bar{a}_i(\bar{a}_i + \bar{a}_j)} = \frac{a_i + \frac{a_i \bar{a}_j}{\bar{a}_i}}{\bar{a}_i + \bar{a}_j} = \frac{a_i + K_{i,j} a_j}{\bar{a}_i + \bar{a}_j}. \quad (7.21)$$

Since

$$(\bar{a}_i + \bar{a}_j) = \text{const.},$$

$$E_{\text{PB}} = \text{const.} + \frac{RT}{z_i F} \ln(a_i + K_{i,j} a_j). \quad (7.22)$$

Note that the charge number of the main and interfering ion are the same.

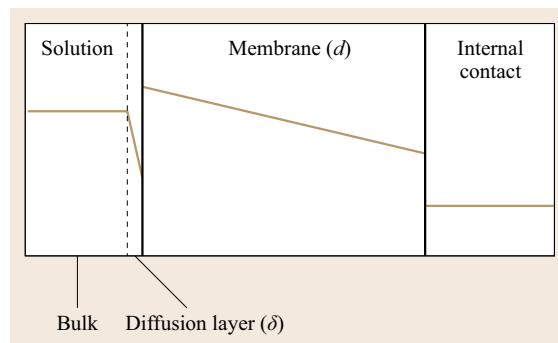


Fig. 7.15 Concentration profiles assumed for the local-equilibrium models (after [7.11])

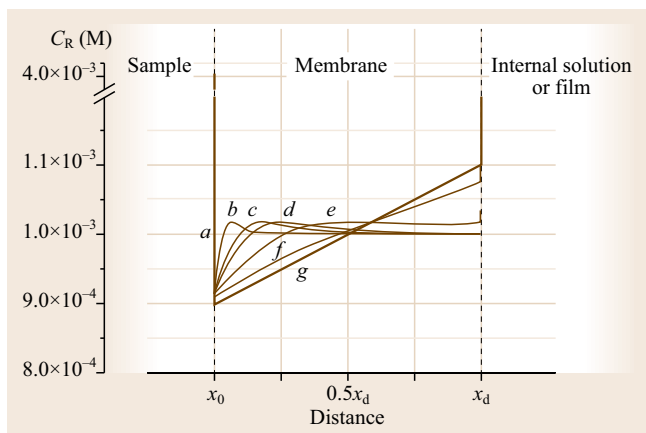


Fig. 7.16 Time-dependent concentration profiles for site R^- ($[i^+] 1 \times 10^{-4}$, $[j^+] 1 \times 10^{-3}$, $D_i/D_j 0.5$, $K_{i,j} 0.1$, and $R_{\text{total}} 1 \times 10^{-3}$). Curves a – g show profiles for: (a) 4×10^{-4} , (b) 1.64, (c) 13.1, (d) 26.2, (e) 104.8, (f) 420, and (g) 13 440 s (steady state) (after [7.12])

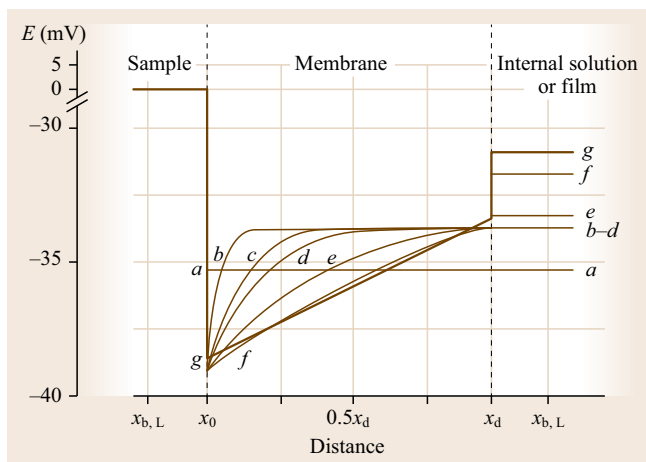


Fig. 7.17 Time-dependent and distance-dependent potential profiles. Curves a – g show profiles after the following: (a) 4×10^{-4} , (b) 1.64, (c) 13.1, (d) 26.2, (e) 104.8, (f) 420, and (g) 13 440 s (steady state) (after [7.13])

Eisenman introduced the migration effect in the phase boundary model. For instance, the equation for the fully dissociated ion exchanger case was derived in the form

$$E_M = E_{PB} + E_D = \text{const.} + \frac{RT}{z_i F} \ln \left(a_i + \frac{\bar{u}_j}{\bar{u}_i} K_{i,j} a_j \right), \quad (7.23)$$

where \bar{u}_i and \bar{u}_j are the mobilities of the respective ions in the membrane.

Despite the simplicity of the total equilibrium model the explicit solution is only possible if the main and interfering ions exhibit the same charge. The often applied Nikolsky–Eisenman equation (7.16) is a (semi) empirical expression, however, it has been proven as very useful in practice. It provides a semiquantitative description of most experiments with ion-selective electrodes and the basis of their evaluation.

Local-Equilibrium Models

In these models, called the diffusion layer models (DLM), ion fluxes result in a steady state concentration profile at the solution–membrane interface. The concentrations depend on the distance perpendicular to the membrane but not on time. See the concentration profile in Fig. 7.15.

Instead of bulk concentrations the local concentrations are used to calculate the potentials. The driving force of the diffusion is the exchange of the main ion and the interfering ion at the solution–membrane interface resulting in a linear concentration profile when the steady state condition is reached. Before the steady state condition is reached potential and selectivity coefficients change with time (Fig. 7.16 and 7.17).

It is predicted that for short readout times the selectivity is a function of the ratio of the diffusion coefficients and not K_{ij} . This can be used for *kinetic discrimination*.

The diffusion layer model was very useful in explaining how poor selectivity and detection limits are caused by increased concentration of the main ion at the membrane surface due to diffusion of this ion from the membrane phase into the solution. *Sokalski et al.* used this approach to find an equation for the detection limit versus concentrations of ions in the inner solution and other parameters [7.13].

The steady state concentration of the main ion at the surface of the membrane is related to the diffusion coefficients of the ion in the membrane and in the bathing solution, respectively

$$c_{io} = c_i + \frac{\bar{D}_i \partial}{D_i d} (c_{io} - c_{id}). \quad (7.24)$$

Figure 7.18 shows the calculated (electro motoric force, EMF) functions for the ISE with the same membrane but different primary ion concentrations in the inner solution. It even predicts the way to improve the detection limit of membrane electrodes.

Advanced Nonequilibrium Methods

Despite the merits of the DLM, the kinetic of the sensor is reduced to the diffusion and the influence of the charge- and field distribution on the motion of ions is

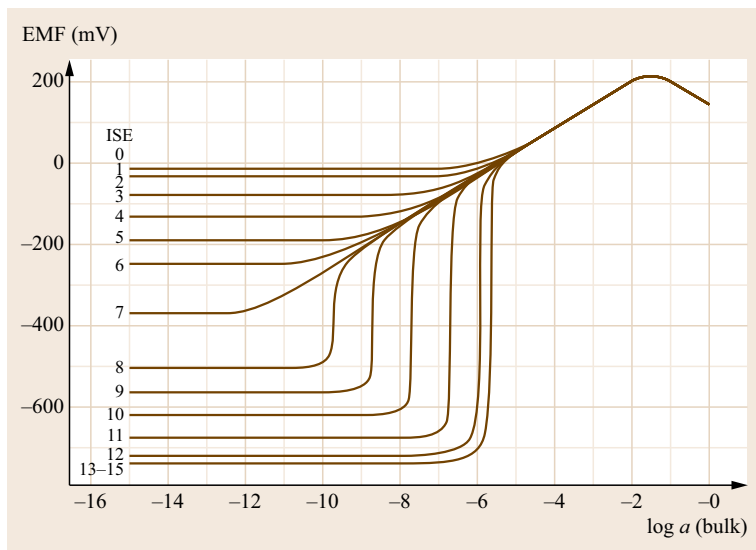


Fig. 7.18 Calculated EMF functions for a series of ISEs having the same membrane but different primary ion concentrations, c_i in the internal solution, from $1-1 \times 10^{-15}$ M in the inner solution. Curves are labeled with the corresponding negative logarithm (after [7.14])

ignored. The advanced nonequilibrium methods omit the idealizing assumptions of the classical models and regard the motions of ions in the membrane and the adhering solutions as a result of the gradients of concentrations and the local electrical fields that are a result of the charge separation. The condition of electroneutrality is no longer presumed and the equilibrium is replaced by reaction rates.

Sokalski and Lewenstam [7.15] used the Nernst-Planck equations to describe the ion fluxes in space (only one dimension perpendicular to the membrane, reduced to the surface area) and time

$$f_i(x, t) = -D_i \left[\frac{\partial c_i(x, t)}{\partial x} - z_i c_i(x, t) \left(\frac{F}{RT} \right) E(x, t) \right], \quad (7.25)$$

where $f_i(x, t)$ is the flux of the i -th ion, $c_i(x, t)$ is the concentration of the i -th ion in space point x and time t , $E(x, t)$ is the electric field, D_i is the diffusion coefficient of the i -th ion, and z_i is the charge of the i -th ion.

The ion fluxes cause an electrical current that is taken into account by the Poisson equation

$$I(t) = F \sum_i z_i f_i(x, t) + \varepsilon \frac{\partial E(x, t)}{\partial t}, \quad (7.26)$$

where $I(t)$ is the total current density and ε is the dielectric permittivity.

The equation system is further completed by mass conservation

$$\frac{\partial c_i(x, t)}{\partial t} = \frac{\partial f_i(x, t)}{\partial x}. \quad (7.27)$$

The kinetic of the ion extraction to and from the membrane is introduced as

$$f_{i0}(t) = \vec{k}_i c_{i,bL} - \overleftarrow{k}_i c_{i,b0}(t), \quad (7.28)$$

$$f_{id}(t) = -\overleftarrow{k}_i c_{i,bR} + \vec{k}_i c_{id}(t), \quad (7.29)$$

where f_{i0} , f_{id} , c_{i0} , and c_{id} are the fluxes and concentrations at $x = 0$ and $x = d$ (where d is membrane thickness), respectively; \vec{k}_i and \overleftarrow{k}_i are the forward and backward rate constants, respectively, and their ratio is a partition coefficient; and $c_{i,bL}$ and $c_{i,bR}$ are the concentrations in the bathing solutions on the left (L) and right side (R) of the membrane, respectively.

The numerical evaluation of this complex system of partial differential equations is easily done in the framework of commercial finite element computer programs.

In principle the advanced models are able to simulate all the effects, known from the practical application of these electrodes, especially the time dependence and distortions of the response curve against the main ion and the course of selectivity and the detection limit.

They are valuable tools in the development of new electrodes and improved analytical protocols. Certainly, as seen from the equations above, the models require more data input for calculation. To get such data as permittivity of the membrane or rate constants of ion partitions requires additional instruments of investigation such as voltammetry and impedance spectrometry. Some results may illustrate the utility of these calculations.

Contrary to the assumptions used in the classical models, the distribution of the ion binding sites in the

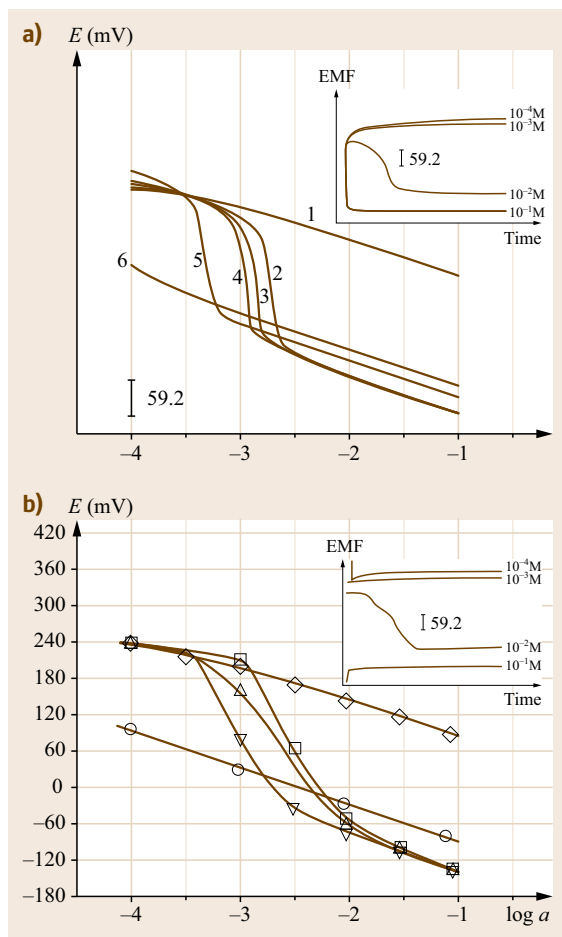


Fig. 7.19a,b Theoretical and experimental calibration curves for the ion-exchanger electrode chloride ion selective sensor (ISS). **(a)** Calibration curves calculated for membrane conditioned in i^- and j^- for solutions of (1) j^- (5 min), (2) i (5 min), (3) i (15 min), (4) i (30 min), and (5) i (60 min), and (6) calibration curve obtained with a membrane conditioned in i^- for a solution of i^- (60 min). i is the preferred ion, and j is the discriminated ion. The inset shows the EMF time dependence for an ISE conditioned in discriminated ion for 1×10^{-4} , 1×10^{-3} , 1×10^{-2} , and 1×10^{-1} M. **(b)** Calibration curves obtained with a membrane conditioned in Cl^- for solutions of Cl^- (5 min/conc.), (O) ClO^- (5 min/conc.), (Δ) ClO^- (15 min/conc.), (□) ClO^- (30 min/conc.). Calibration curve obtained with a membrane conditioned in ClO^- for a solution of (O) ClO^- (60 min/conc.) ClO_4^- is the preferred ion, and Cl is the discriminated ion. The inset shows the EMF time dependence for an ISE conditioned in Cl^- for 1×10^{-4} , 1×10^{-3} , 1×10^{-2} , and 1×10^{-1} M (after [7.16])

membrane is not constant in space and time, but the ion exchange between the bathing solution and the membrane causes at first a nonlinear profile of the binding sites and only after 7 min is a nearly linear profile reached, (Fig. 7.16).

Whereas in equilibrium models the potential in the membrane is assumed to be locally independent, the advanced theory enabled the potential distribution across the membrane and its dependence on time. The total potential of the electrode corresponds to the integral of the local potential over the membrane

$$E_M(x, t) = \int_{x_{b,L}}^{x_{b,R}} E(x, t) dx, \quad (7.30)$$

where $x_{b,L}$ and $x_{b,R}$ are the points in the bulk of bathing sample solution (on the left, L) and internal solution/film (on the right, R).

The nonideal behavior of ion-selective electrodes in solutions with an interfering ion is illustrated in Fig. 7.19, where a pretreatment of the electrode with the interfering ion results in a change of the response curve. The comparison of calculated and measured curves proves that the advanced model adequately describes the processes inside the ISE.

7.1.7 All Solid-State Electrodes

To overcome the barrier between the ion conducting membrane and the electron conducting metal and to prevent polarization at the interface, a reversible redox system or a high capacitive layer must be inserted between the metal and the membrane. The conductive organic polymers such as polypyrrol, polyanilin and polythiophene derivatives offer a very convenient transition from electrons to ions (Fig. 7.20). The polymers directly grow from a solution of the monomers on an inert electrode by electrochemical oxidation. Further oxidation generates cationic sites and the corresponding amount of anions is intercalated in the layer.

Thus the uptake of an anion results in a transfer of an electron to the metal and vice versa. The capacity of these polymers is high enough to prevent potential shifts in the case of a low current. The stability of this kind of redox layer is limited by side reactions such as the reaction with oxygen and chemical degradation. If water penetrates the membrane it sometimes destroys the contact between the membrane and the conducting polymer, forming an additional layer; instable interface potentials and a bad performance of the electrode are the consequences. In an effort to optimize these types of all solid-state electrodes a variety of conducting poly-

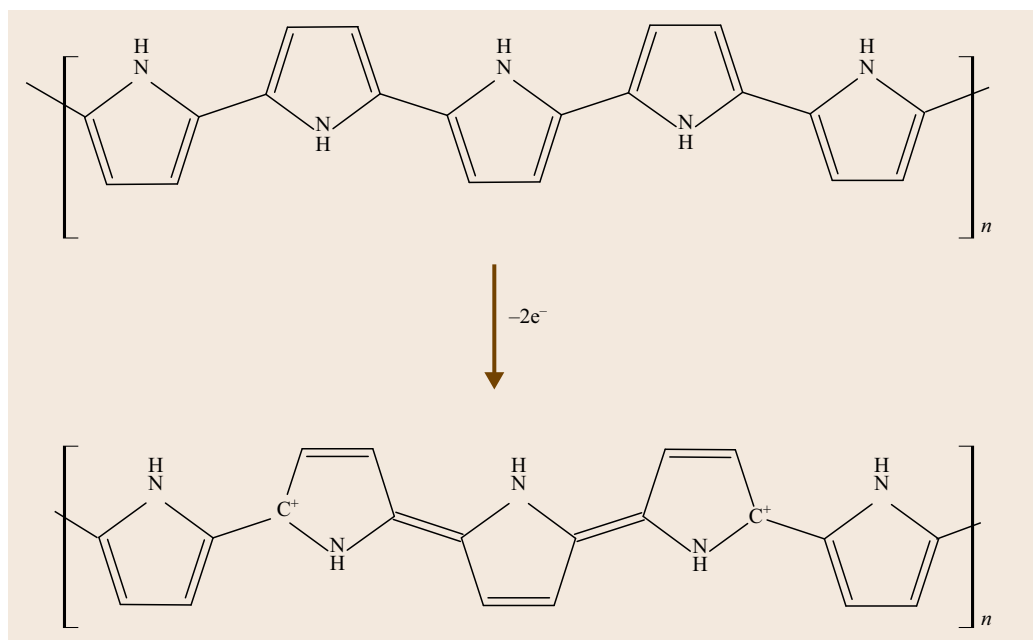


Fig. 7.20
Polypyrrole after polymerization; the polypyrrole is stepwise further oxidized yielding radical cations and dication

mers have been tested. Some examples are given in Fig. 7.21.

Good performance was achieved with polymerized thiophene derivatives such as Poly(3-octyl thiophene) (POT, formula given in Fig. 7.21c), which is highly lipophilic and prevents the inclusion of water. Besides the electrochemical grafting the polymer can be dissolved in organic solvents and easily casted onto the metal. As the ion exchange in the conducting polymer in principle is the same as in the overlaying ion-selective membrane, it is also possible to omit the plastic membrane and to incorporate the ion-recognition sites in the conducting polymers as immobilized doping ions. The polymers themselves are used as sensing membranes. On the other side soluble redox polymers have been added to the membrane forming a cocktail to ensure electron transfer in coated wire electrodes. As the redox active polymer comes in direct contact with the sample solution such electrodes are sensitive against redox active agents in the sample.

Another approach to facilitate the ion-electron charge transfer is to enhance the double layer capacity at the interface. This is achieved by the application of carbon black, carbon nanotubes, graphenes, fullerene and other conducting nanoparticles at the interface between the electronic conductor and the membrane. This technique has already been established in the construction of supercapacitors.

All these developments not only bear the possibility of miniaturization, but even the mass production of in-

expensive sensors by highly automated processes such as ink jet printing of the sensor materials onto paper, plastics or ceramic [7.17]. All techniques developed for the production of electronic printed boards as well as integrated circuits have been tried as platforms for the preparation of ion-selective electrodes and arrays of them even in combination with other sensors and micro-mechanics. These sensors are compatible with flow analyzers and micro analytical systems (μ -TAS (total analytical system)).

Beside the indicator electrode the complete sensor system needs an adequate reference electrode. This part of miniaturized sensors causes the most troubles and is often neglected.

The classical silver/silver chloride system often incorporated in a gel and covered by a porous membrane can be used. A plasticized PVC reference membrane containing equimolar amounts of both cation and anion-exchanger, potassium tetrakis (4-chlorophenyl) borate and methyltri-dodecylammonium chloride, together with solid potassium chloride and silver chloride with traces of silver over a polymer conductive layer was proposed [7.6].

Depending on the analytical problem, instead of a conventional reference electrode the voltage is alternatively measured against a second ISE. If the sample is buffered to a constant pH, then a pH sensor is a suitable reference. A constant chloride ion concentration allows a Cl^- Sensitrode as reference. In flow systems it is possible to use identical ISEs, one flushed with a standard solution, the other with the sample.

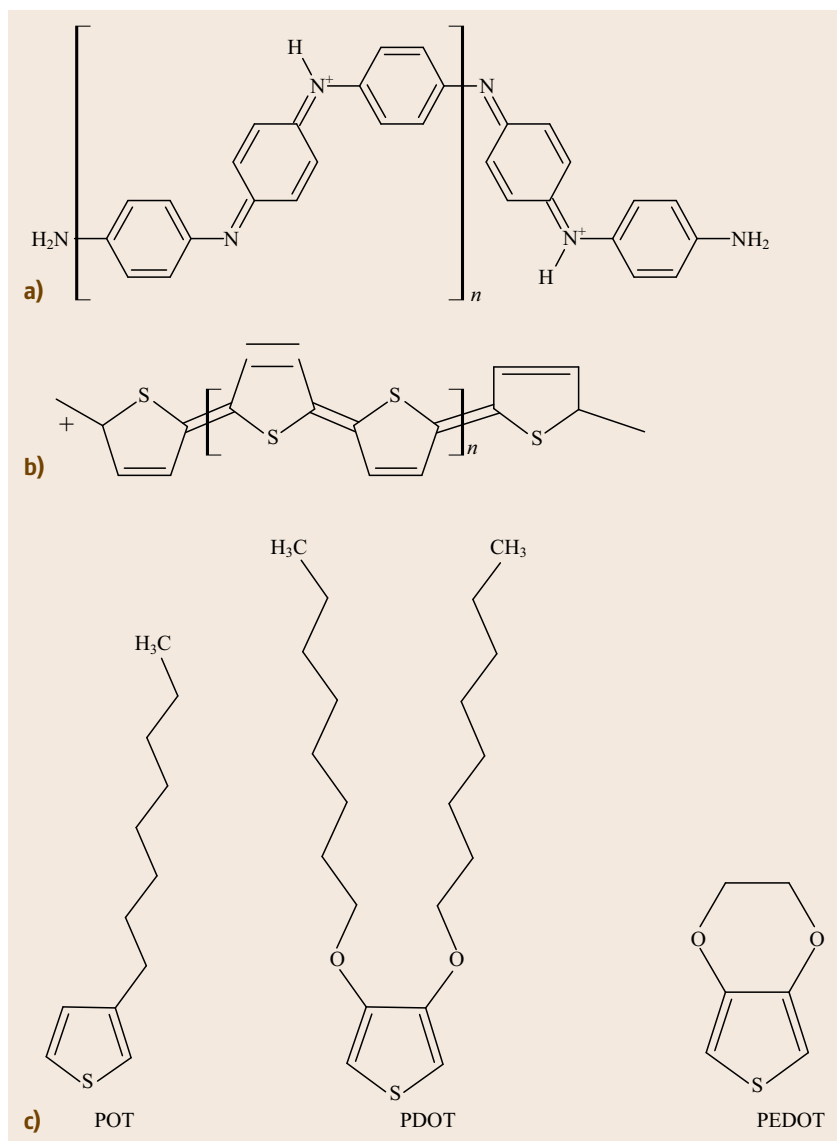


Fig. 7.21 (a) Polyaniline; (b) Polythiophene and (c) Monomer units of conducting thiophene polymer derivatives

Table 7.6 Selection of drug responsive membrane electrode (after [7.15])

Drug	Exchanger	Sample or uses
Amitriptyline	Amitriptyline tetraphenylborate	Response studies
Metoclopramide	Metoclopramide tetraphenylborate	Pharmaceuticals
Amphetamine	Amphetamine dibenzo-crownethers	Selectivity studies
Berberine	Berberine bromomercurate	Tablets
Berberine	Berberine tetraphenylborate	Response studies
Naproxen	Tetraheptylammonium naproxenate	Tablets
5,5 diethylbarbiturate	Tetraoctylammonium 5,5 diethylbarbiturate	Response studies
Cocaine	Cocaine dipicrylaminat	Response studies
Salicylate	Derivatized porphyrine tin dichloride	Biological samples
Benzylpenicillin	Benzyltrimethylcetylammmonium-benzylpenicilline	Pharmaceuticals
Nicotine	Nicotine tetraphenylborate	Tobacco products
Scopolamine	Scopolamine tetraphenylborate	Response, selectivity studies

7.1.8 Ion-Selective Field Effect Transistor (ISFET)

Already 40 years ago *Bergveld et al.* placed the ion-selective membrane directly at the input transistor of the voltmeter [7.18]. The input stage of most voltmeters uses field effect transistors (FET) to ensure the high input resistance. Figure 7.22 shows the scheme of a FET linked to an ion-selective electrode.

Usually the gate electrode of the FET is connected to the ISE and reference electrode is connected to the bulk contact. The voltage between the bulk and the isolated gate electrode generates an electric field in the tiny channel below the gate and controls the current between source and drain electrode. Placing the ion-sensitive layer directly above the gate insulator removes all the capacities of the cables and connectors in between, thus the charge that must be transferred following a change of the potential is drastically reduced. This should result in a much better dynamic response and a lower polarization of the membrane–gate interface. Another advantage of the direct capacitive coupling of the ion-selective layer to the gate insulator is that even imperfect layers with holes, which would cause a short cut in conventional ISE, provide a suitable response. Fluoride sensitive FETs have been produced by vapor deposition of LaF_3 resulting in a nonperfect layer with holes, but that worked perfectly [7.19]. The low output impedance of the transistor prevents the uptake of *electrosmog* and disturbance by electrostatic charges. There are two operation modes using ISFETs:

1. Registration of the source-drain-current. This current is a nonlinear function of the gate potential (Fig. 7.23) and additionally depends on the temperature.
2. The drain current is regulated by an operational amplifier as shown in Fig. 7.24 to a constant value by compensating for the potential difference at the sensing layer by an additional voltage, which is introduced between the reference electrode and the sensor. Here the voltage just corresponds to the potential of a conventional ISE.

The concept of the ion-selective field-effect transistor (ISFET), the link between the very progressive tech-

Fig. 7.24 Schematic circuit of constant drain current operating mode with negative feedback to the reference electrode. The current is set by the resistor, which just compensates the current from the ISFET at the inverting input of the operational amplifier. The output voltage results the potentiometric function of the ISFET ▶

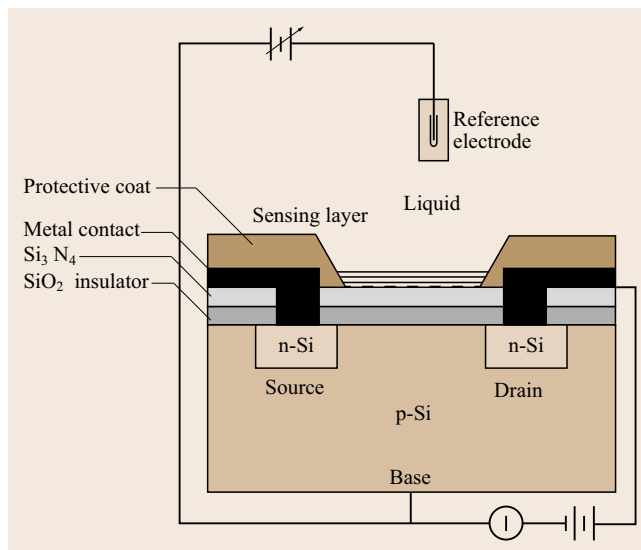


Fig. 7.22 ISFET, ion-selective field-effect transistor

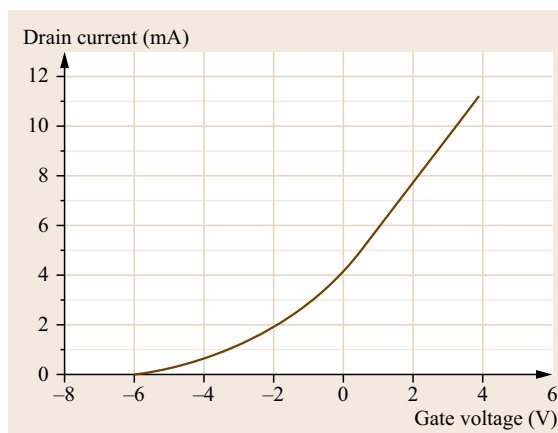
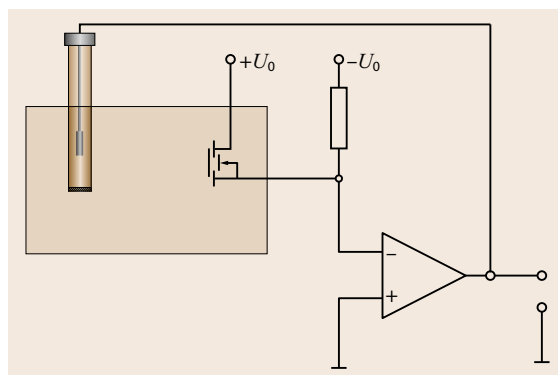


Fig. 7.23 Response function of an-n-channel depletion FET



nique of microelectronics and electrochemical sensing was and is indeed very alluring, but electronic devices are not compatible with water. Except for the sensing layer all other parts must be insulated from the medium. This problem was solved by placing the contacts to the backside and isolating the rest with SiO_2 . As in the case of the early *coated wire electrodes* the interface between the membrane and the gate isolator is not well defined. This disadvantage may be resolved by interlayers of conducting polymers or carbon nanotubes as in the all solid-state electrodes. A FET is not an ideal device. In integrated circuits for ionometers all these disadvantages are internally compensated. Therefore the ISFETs did not replace the conventional ISE.

7.2 Application of ISE

Besides the visual pH strips that allow an estimation of the pH value, the majority of the more exact pH measurements in the laboratory are done with pH meters. This is a standard instrument not only in chemical labs, but also pharmaceutical and biological labs. Small electronic pH sticks also contain a glass electrode as a sensing element. It is very easy to replace the pH electrode against another ISE, switch the pH scale to the mV display and do the job.

To get reliable results, selectivity and working range must be checked, and depending on the analytical problem sample preparation and calibration has to be performed. An abundance of suitable analytical protocols can be found in the application notes of the electrode manufacturers [7.10].

For the determination of concentrations the ion strength must be adjusted to the same value for sample and calibration standards and the measurements should be carried out at the same temperature. The electrodes are dipped into the solution and under gentle stirring a stable readout should be arrived at after a few minutes. Continuous drift indicates a failure of the system, often of the reference electrode. If the voltage fluctuates, then the conductivity of the sample is too low or the liquid junction of the reference electrode is clogged. The temperature dependence of the ISE according to the Nernst equation is compensated for in most instruments by a built-in thermometer or the temperature is set manually.

Some comfortable instruments often combined with titrators allow the automation of the whole analytical procedure, including the calculation of the analytical result. After usage the electrode has to be cleaned by distilled water and stored under appropriate conditions.

7.1.9 Drug Sensitive Electrodes

The majority of drug molecules bear a basic or acidic function and they are ionized at a suitable pH. The corresponding ions are comparably lipophilic and interact with an ion exchanging membrane. Some drug sensitive electrodes have been constructed for special purposes such as response studies. Contrary to the more complex and only intermittent registration methods such as high performance liquid chromatography (HPLC), the ISE allows for continuous monitoring. Table 7.6 gives some examples of drug sensitive electrodes.

Molecular imprinted polymer membranes promise further progress in selectivity of drug molecules and other xenobiotics.

To compensate for drift, a one-point calibration should be performed before, between and at the end of a series of samples. From time to time the slope has to be checked.

Specialized analyzers such as the AVL 9180 Analyzer for clinical analysis of the electrolytes in blood and urine are equipped with an assembly of flow-through electrodes for K^+ , Na^+ , Ca^{2+} , pH and Cl^- . These *fool proof* instruments contain self-checking programs that flush the salt bridge of the reference electrode, clean the system and calibrate the electrodes.

Almost all titrations benefit from electrochemical end point detection. It is beyond the scope of this chapter to deal with the numerous variants of potentiometric titrations from acidimetric, redox and complexometric titrations. Chloride-ISEs are used for argentometric titration and Ca-ISE for complexometry. The titration of ionic tensides or ionic biopolymers is demonstrated with tenside electrodes.

7.2.1 Gas-Sensitive Electrodes and Biosensors

An interesting extension of the application of ISEs is achieved by attaching a further reaction layer onto the ion-selective membrane. A thin buffer solution layer in front of a one-rod pH sensor, separated by a (silicone) rubber membrane, which allows the penetration of reactive gases such as CO_2 or NH_3 results in a gas-sensitive electrode. Between the partial pressure of CO_2 for instance and the pH of the carbonate/bicarbonate buffer a secondary equilibrium is established that enables the direct measurement of the partial pressure of CO_2 . A typical application is the blood gas analyzer.

The ammonia-sensitive electrode reads the ammonium after alkalization and has found applications in the determination of urea, which is converted by urease to ammonia.

As opposed to a gas-permeable membrane, the separation of the sample solution is also possible simply by placing the electrode above the sample. Then the gas diffuses through the gap between the meniscus of the sample and the electrode.

Highly specific enzyme reactions bound in a layer above the ion-selective membrane producing any detectable species are used as biosensors. The enzyme reaction results in a steady state between product formation and diffusion of this product from the electrode. As the enzyme reaction requires distinct conditions related to temperature, pH and coenzyme concentration the concept of the enzyme electrode seems to be overloaded to some extent. For routine analysis such electrodes are used as disposable sensors or are prepared occasionally on the bench. The stability of the enzymes except from a few cases is very limited, therefore the sensor should be stored in a refrigerator.

Instead of pure enzymes, even small organisms such as bacteria, yeast or algae, different tissues, and parts

of cells such as mitochondria have been placed at the sensing site of an ISE.

Immune reactions are indicated using the concept of the enzyme-linked immunosorbant assay (ELISA). The Immune reaction results in an immobilization of the linked enzyme in front of the electrode and the product of the enzymatic reaction is detected. Sometimes nonnatural substrates are used, such as 4-fluorphenol, which releases fluoride upon oxidation, which is sensed by a fluoride electrode.

7.2.2 Detectors in Flow Systems

Flow systems offer a wide variety of automated sample preparation, as HPLC or capillary electrophoresis, dilution or reactions as in flow injection analysis are compatible with ISEs. Their response is independent of the sample volume enabling miniaturization to save reagents and avoid waste.

Some examples are flow injection determination of total concentration of aliphatic carboxylic acids [7.20]; application of a potentiometric electronic tongue in food analysis [7.21]; or a potentiometric detector in capillary electrophoresis [7.22].

7.3 Amperometric and Voltammetric Methods

A current flowing through an electrode disturbs the equilibria at all interfaces between different phases. Particularly at the interface between electronic conductors and ionic conductors, the transition of electrons involves oxidation in the case of positive (anodic) or reduction in the case of negative (cathodic) charge transfer.

The current corresponds to the reaction rate according to Faradays law

$$\frac{dn}{dt} = \frac{1}{zF} \frac{dQ}{dt} = \frac{1}{zF} I. \quad (7.31)$$

As a heterogeneous reaction the rate is proportional to the area of the electrode where the reaction takes place. As the reaction goes on, the concentration of the educt is depleted at the surface and as a consequence the concentration of the product increases. This causes a concentration gradient near the electrode and forces diffusion of the educt to the electrode and the product from the electrode. If the charge transition is not kinetically hindered, then these transport phenomena control the current, and the potential at the *working* electrode corresponds to the actual surface concentrations of the redox couple according to the Nernst equation.

7.3.1 Experimental Methods

The experimental setup is a little bit more complex than in simple open circuit potentiometric measurements. Although most reference electrodes are stable against small currents it is better to avoid a current through the reference electrode. Therefore an auxiliary electrode as a third electrode is introduced. The current then flows between the auxiliary and the working electrode, while the potential at the working electrode is measured against the reference electrode with a high impedance voltmeter.

The inner resistance of the solution causes an ohmic drop, resulting in a potential error.

To counteract this error the reference electrode is placed as near as possible to the working electrode, using a Luggin capillary and the conductivity of the electrolyte is increased by addition of a suitable inert salt. The current is kept low, using a small working electrode. With these small working electrodes the electrochemical conversation related to the bulk of the solution can be neglected.

Different measuring regimes have been established so far.

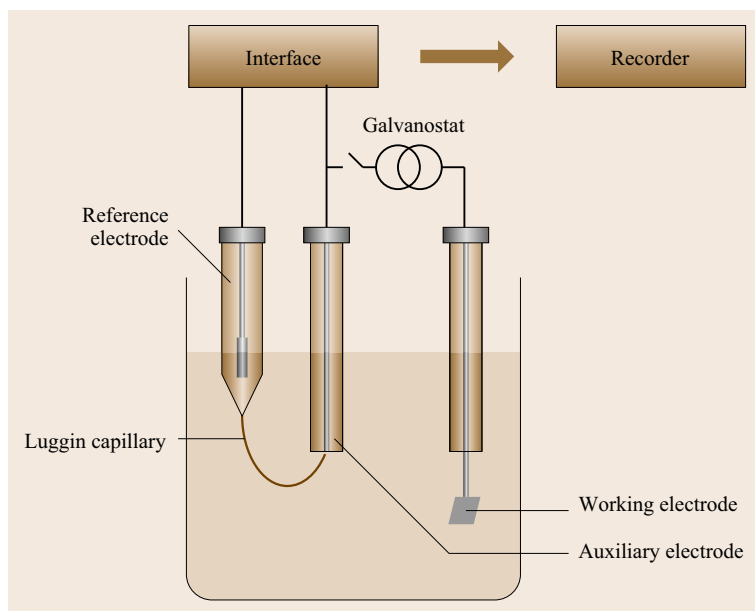


Fig. 7.25 Experimental setup of chronopotentiometry

Quiet solution, no convection:

- *Chronopotentiometry*: Current is switched on, regulated to a constant value, potential is recorded as function of time
- *Chronoamperometry*: Potential is stepped to a defined value, current is recorded as function of time
- *Linear sweep voltammetry*: Potential is set as a linear function of time, current is recorded as function of potential
- *Cyclic voltammetry*: Potential set as a triangular function of time, current is recorded as function of potential.

There are several variants of voltammetry with more complex potential time functions, such as staircase voltammetry, pulse voltammetry, AC-voltammetry, and stripping voltammetry.

Forced convection:

- *Polarography*: Dropping mercury electrode
- *Rotated disk electrode*
- *Vibrated disk electrode*: Current is recorded as function of potential
- *Streaming solution*: In flow injection analysis and HPLC detectors, current is recorded as function of time or potential
- *Chronopotentiometry*.

The procedure may be illustrated in a simple system. The cell is equipped with a platinum disk working electrode, 3 mm diameter sealed in glass. Prior to usage the electrode is polished with fine ground alumina and

carefully cleaned with a mixture of concentrated sulfuric acid and hydrogen peroxide. As shown in Fig. 7.25 the cell is further completed with an auxiliary platinum electrode and a silver/silver chloride reference electrode.

The cell is filled with 1 M KCl and 1 mM potassium hexacyanoferrat (II) in water. The potential is measured with a high-impedance voltmeter interfaced to a computer recording the potential time function. The current is generated by an electronic current source *galvanostat* and adjusted to $+100 \mu\text{A}$.

As the current is switched on, the hexacyanoferrat (II) begins to be oxidized at the electrode to hexacyanoferrat III. Since the coordination sphere of the iron atom is not changed and the charge can be easily distributed, this reaction is almost quick and reversible. The potential of the working electrode is shifted to a positive direction and when almost all of the reduced species is consumed at the surface of the electrode a steep increase in the potential is observed. This point of time is called the *transition time* (τ). Since the current is kept constant anything else must be oxidized; here the chloride of the ground electrolyte is oxidized to chlorine at the end. Provided that any convection during the measurement is prevented and the conductivity of the solution is kept high, the transport of the reduced and oxidized species is governed by a planar diffusion perpendicular to the active surface of the electrode. This can be described by Fick's second law

$$\frac{\partial c}{\partial t} = D \frac{\partial^2 c}{\partial x^2} \quad (7.32)$$

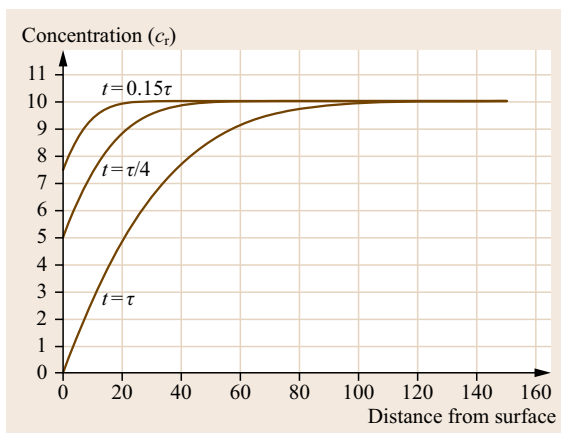


Fig. 7.26 Evolution of concentration gradients at the surface of the working electrode after the current is switched on

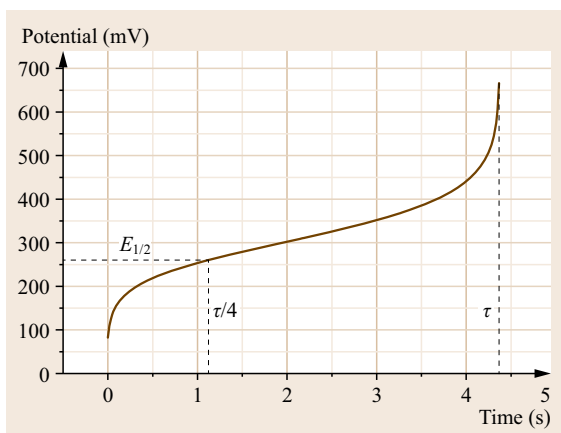


Fig. 7.27 Chronopotentiometric record of the oxidation of hexacyanoferrate (II)

As long as the educt is not exhausted, the oxidation goes on at the surface with a constant rate according to (7.31) and the depletion of the of the hexacyanoferrate (II) extends more and more into the bulk solution, as illustrated in Fig. 7.26.

In the case of a reversible quick reaction the measured potential is determined by the Nernst equation and the standard potential is reached when just the half of the reduced form is oxidized. This is the case at a quarter of the transition time (Fig. 7.27). Solutions of the differential equations (7.31) and (7.32) reveals that the square root of the transition time is proportional to the bulk concentration

$$\tau^{1/2} = \frac{\pi^{1/2} z F D^{1/2}}{2i} c_r. \quad (7.33)$$

For simplicity diffusion coefficients of reduced species as well as the activity coefficients are set to be equal.

The current density must be adapted to the concentration to ensure a transition time of a few seconds to avoid onset of spontaneous convection and deviation from planar diffusion. Therefore this old procedure by *Karaoglanoff* [7.23] is seldom used in analytical practice.

Chronoamperometry

In all amperometric or voltammetric methods the potential of the working electrode is set to a defined value. This is done by an electronic controller, the potentiostat. Usually a potentiostat is realized with an integrated operational amplifier. Such amplifiers exhibit a differential input and a high open loop gain of about 1×10^5 . A typical schematic setup is shown in Fig. 7.28.

The nominal potential is set at the potentiometer or a digital-analog-converter from a computer. Because of the high amplification of A1, the voltage of the auxiliary electrode is regulated to an appropriate value, which ensures an input difference at A1 near zero. This means that the potential of the reference electrode against ground is just the set voltage. The second amplifier holds the potential of the working electrode at ground and the output voltage of A2 corresponds to

$$U_{\text{out}} = -RI_{\text{in}}. \quad (7.34)$$

The feedback resistor must be adapted to the expected current to ensure a suitable working range of the amplifier and the recorder. There are some other more sophisticated schemes on the instruments market to meet special demands for high regulation speed or higher currents.

Let us consider again a reversible diffusion controlled oxidation, without any complication.

Switching the potential from about 150 mV below the redox potential to a value 150 mV above the standard potential results first in a sharp peak of current to charge the double layer of the working electrode. This capacitive current exponentially decays, depending on the conductivity of the solution. The new potential corresponds to a ratio of $c_{\text{ox}}/c_{\text{red}}$ of about 0.997. The surface concentration of the reduced species is near zero and a concentration gradient evolves from the surface into the solution. Figure 7.29 shows the concentration profiles $c_{\text{red}}(x, t)$ calculated from Fick's second law with the boundary conditions of $c_{t=0} = c_B$ and $c_{x=0} = 0$.

The solution of the differential equation yields

$$c_{\text{red}}(x, t) = c_L \operatorname{erf}\left(\frac{x}{2D^{1/2}t^{1/2}}\right), \quad (7.35)$$

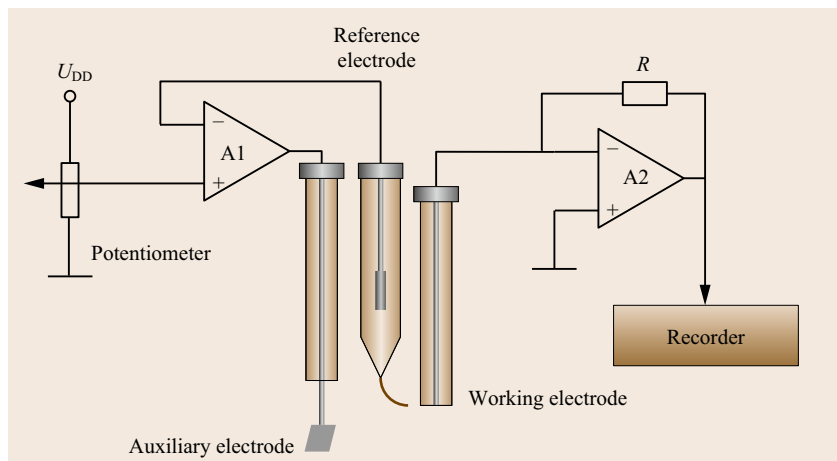


Fig. 7.28 Potentiostat

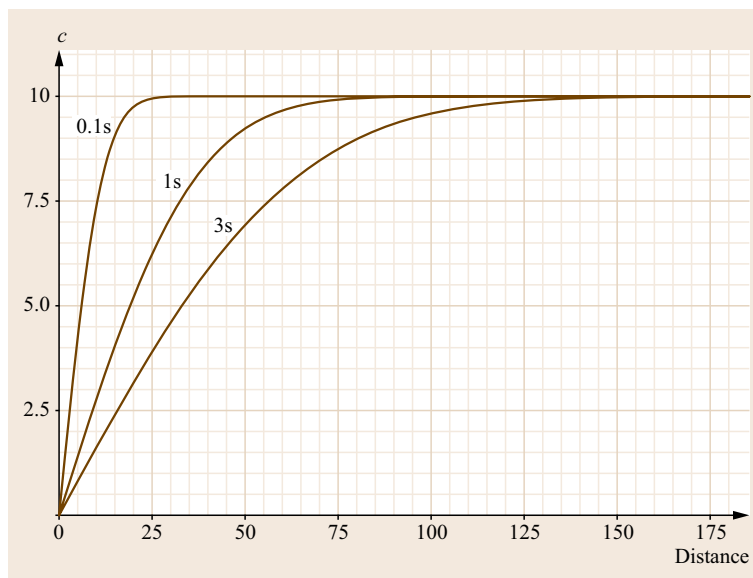


Fig. 7.29 Concentration profile near the surface of the electrode during the chronoamperometric experiment, calculated following (7.35)

where erf = error function.

The current density j decays with the square root of the time

$$j = \frac{zFD^{\frac{1}{2}}c_L}{\pi^{\frac{1}{2}}t^{\frac{1}{2}}} \quad (\text{Cottrell equation}). \quad (7.36)$$

Plotting $1/j$ against the square root of time yields a straight line from which the diffusion coefficient conveniently may be derived. Deviation from linearity is indicative of a more complicated kinetic.

Linear Sweep Voltammetry

The experimental setup is just the same as in chronoamperometry, but the set potential is swept with time. A wide variety of potential time functions are used in

the practice of electrochemical measuring techniques. Rectangular, sawtooth or staircase functions, linear ramps with overlaid Sin of different frequencies and pulses are used. Linear sweep voltammetry we discuss here to show the principal phenomena. In a typical oxidation experiment we start far below the redox potential and increase the potential with a constant voltage rate. The response curve is shown in Fig. 7.30. A small, ideally constant, current is recorded due to the charging of the double layer. It is proportional to the sweep rate

$$I = Cv, \quad v = \frac{dU}{dt}. \quad (7.37)$$

Near the redox potential the oxidation begins, resulting in a Faraday current reaching a maximum above the

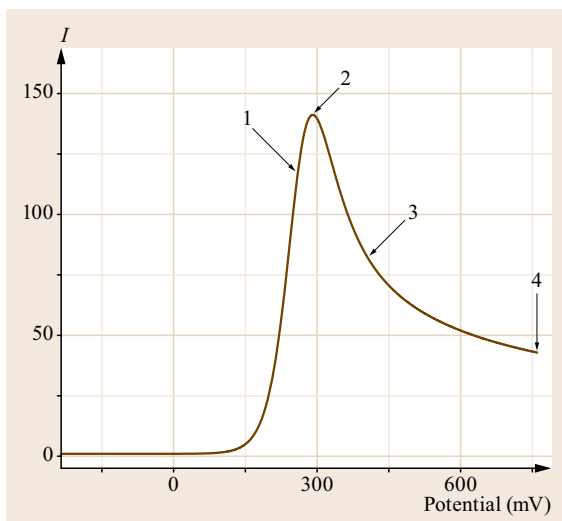


Fig. 7.30 Single-sweep voltammogram, pure diffusion control

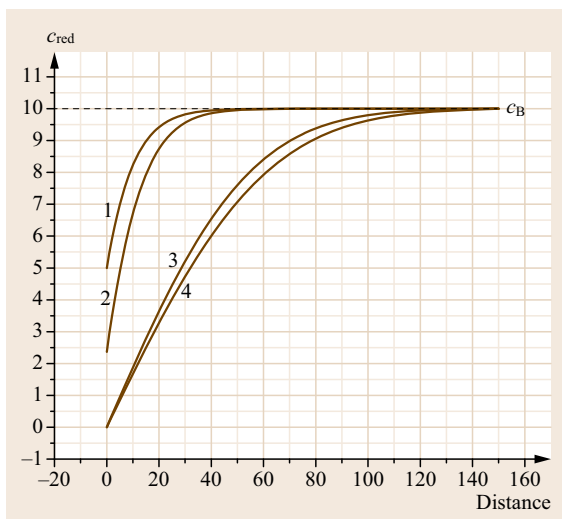


Fig. 7.31 Concentration profile at single-sweep voltammogram

standard potential (7.1) and then decays as the surface of the electrode is depleted of reactive material.

The current decay obeys the square root law as in chronoamperometry. The surface concentration is already zero at point 3 and 4 in Fig. 7.30.

Compare the concentration profiles in Fig. 7.31.

The peak current density is proportional to the bulk concentration and the sweep rate

$$j_p = 2.69 \times 10^5 z^{\frac{3}{2}} D^{\frac{1}{2}} c_L v^{\frac{1}{2}} \quad (7.38)$$

(Randles-Sevcik equation),

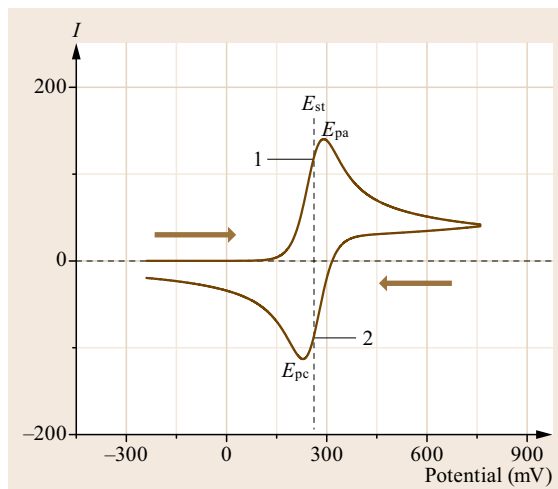


Fig. 7.32 Cyclic voltammetry of a reversible one-electron oxidation

where j_p in $A\ cm^{-2}$, D in $cm^2\ s^{-1}$, c in $mol\ cm^{-3}$, v in $V\ s^{-1}$.

The sweep rate ranges from some millivolts per minute to $1000\ V\ s^{-1}$. At very slow sweep rates the convection is difficult to avoid and at high sweep rates the capacitive current (7.37) becomes much higher than the Faraday current. The peak potential does not depend on sweep rate in a pure diffusion-controlled electrode reaction. If any other kinetic effects are involved then a distinct dependence of the peak potential from the sweep rate is observed and the shift of the peak potential serves as diagnostic criteria for a variety of reaction mechanisms. It even provides the kinetic constants.

Cyclic Voltammetry

Much more information can be acquired when the linear sweep is extended, reversing its direction at least after the peak and scan back to the starting potential. This results in a triangular potential time function. In our example the oxidized product of the first positive part of the scan is then reduced again. Because of diffusion, both peaks are separated by 59 mV in the case of a reversible one-electron transition.

The standard potential (points 1 and 2 in Fig. 7.32) situates just in between the two peak potentials

$$E_{st} = \frac{E_{pa} - E_{pc}}{2}, \quad (7.39)$$

where, as the forward part equals the single sweep, there are quite different concentration patterns for the reverse scan at the same potential.

With additional scan cycles a steady state is reached producing nearly identical voltammograms. If only

a few parts of the electrochemical product decay, then the educt is only partly regenerated at the reverse scan and disappears after some time. As the peak current is proportional to the bulk concentration (Fig. 7.33), it is possible to use single sweep or cyclic voltammetry for analytical determination of concentrations, but a much more important application of the method is the investigation of electrochemical reaction mechanisms. The researcher now has a well-developed theoretical background as well as powerful computer programs at hand to interpret the data from cyclic voltammetry. Nevertheless any voltammetric experiment must be carefully designed to avoid distortions of the potential by IR (voltage) drop or undesired blocking of the electrode surface.

The investigation of reaction kinetics needs the application of a wide range of scan rates. At high scan rates the use of microelectrodes ensures low current and thus minimizes the IR drop and capacitive current. When the diameter of the active electrode becomes smaller than the extension of diffusion layers before the surface, then the condition of planar diffusion no longer holds.

Microelectrodes

Typical disk microelectrodes have a diameter from 1–100 μm but there are even downsized ultra microelectrodes in the nanometer range. A spherical diffusion field governs the transport at a microelectrode. Theoretical treatment results in a time-independent additional term of the Cottrell equation

$$j = \frac{zFD^{1/2}c_L}{\pi^{1/2}t^{1/2}} + \frac{zFDc_L}{r} \quad (7.40)$$

At very small electrodes this term is decisive and results in a constant and much higher current. The current itself is relatively low in the pA to nA range. To improve the signal to noise ratio it is also possible to use a bundle of microelectrodes in parallel. The constant diffusion to the surface results in a sigmoid form of a voltammogram as shown in Fig. 7.34. Ferrocen is reversibly oxidized in a solution of 0.1 M tetraethylammonium tetrafluoroborate as a conducting electrolyte resulting a typical voltammogram at the macroelectrode but a sigmoidal voltammogram at a microelectrode. Very small microelectrodes are used in electrochemical microscopy.

Electrochemical Kinetic

Charge transfer from an electrode through the double layer to a molecule in the electrolyte needs some activation energy and the change of its oxidation state involves transformation of bonds in the molecule. These

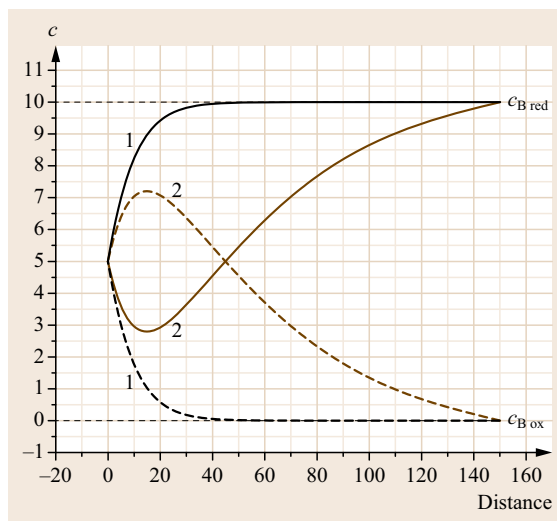


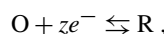
Fig. 7.33 Concentration profiles at the working electrode during cyclic voltammetry (CV) experiment, *black* forward scan, *brown* backward scan

processes take some time and if the rate of the electron transfer is slower than the diffusion, the current is controlled by the reaction rate rather than by diffusion.

The activation energy of a chemical reaction determines the temperature dependence of its rate constants according to the Arrhenius equation

$$k = Ae^{-\Delta G^\ddagger/RT} \quad (7.41)$$

In the case of an electrochemical reaction,



the charge transfer across the phase boundary results in an additional electrical energy $zF\Delta E$, which contributes not only to the free energy of the equilibrium reaction but even to the activation energies of the forward and backward reactions.

At equilibrium potential, both anodic and cathodic reaction rates are the same and as the frequency factor A is independent of the direction of the reaction the activation energies are equal too.

A deviation from the equilibrium potential in the positive direction accelerates the oxidation, decreasing its activation energy by a fraction $(1 - \alpha)$ of the electrical energy

$$\Delta G_a^\ddagger = \Delta G^\ddagger - (1 - \alpha)zF(E - E^0).$$

In contrast the activation energy of the reduction increases by the remaining fraction

$$\Delta G_c^\ddagger = \delta G^\ddagger + \alpha zF(E - E^0), \quad (7.42)$$

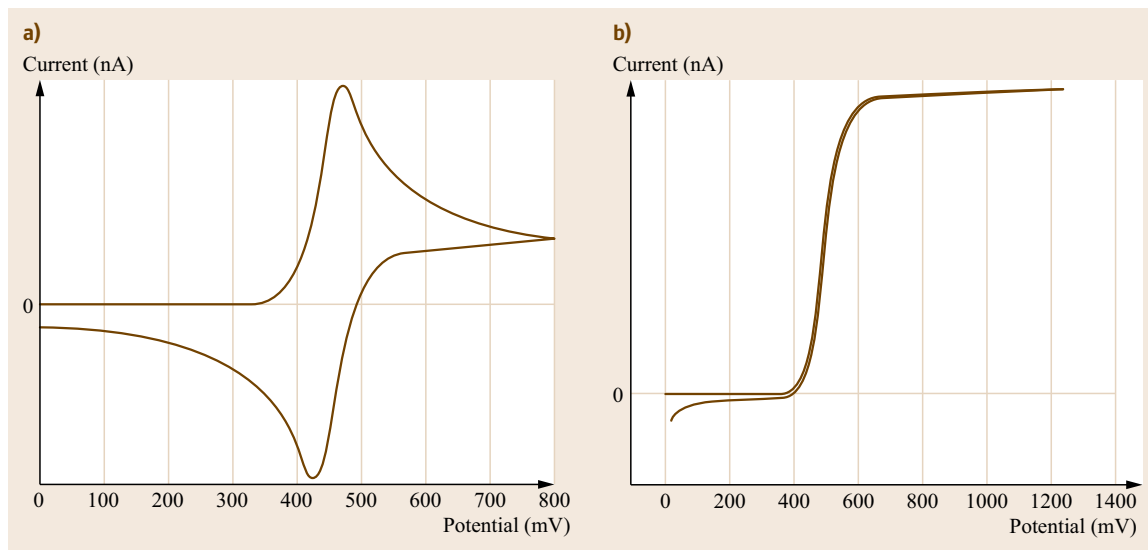


Fig. 7.34a,b Cyclic voltammetry of ferrocen (**a**) At a platinum disk electrode, diameter = 1 mm and (**b**) $d = 10 \mu\text{m}$ (currents not to scale)

where α is the transfer coefficient. It typically ranges from 0.2–0.8.

Introducing the electrical terms into the Arrhenius equation results in

$$k_a = A e^{+[\Delta G^\ddagger - (1-\alpha)zF(E-E^0)]/RT},$$

$$k_c = A e^{-[\Delta G^\ddagger + \alpha zF(E-E^0)]/RT},$$

summarizing the potential independent term in k^0

$$k_c = k_c^0 e^{-\alpha zF(E-E^0)/RT}$$

and

$$k_a = k_a^0 e^{(1-\alpha)zF(E-E^0)/RT}.$$

The reaction rate relates to the current density as

$$j = zFkc.$$

At equilibrium, where $E = E^0$, both current densities are the same, and the anodic and cathodic current compensate each other. Its absolute value, representing the dynamic of the equilibrium is called exchange current density

$$k_c = k_a = k^0, \quad j_0 = zFk^0c \text{ for } (c = c_O = c_R).$$

At potentials away from the equilibrium, the net current density is given by the Butler–Volmer equation

$$j = zFk^0(c_R e^{(1-\alpha)zF(E-E^0)/RT} - c_O e^{-\alpha zF(E-E^0)/RT}),$$

inserting j_0 at equivalent concentrations of O and R,

$$j = j_0(e^{+(1-\alpha)zF(E-E^0)/RT} - e^{-\alpha zF(E-E^0)/RT}).$$

The potential difference in the exponent is called overvoltage η . At an overvoltage of about 100 mV the cathodic current density vanishes and a plot of $\ln(j)$ against η results in a slope of $(1-\alpha)zF/RT$ from which α can be derived. Analogously, at negative potentials only the cathodic current remains relevant (Fig. 7.35).

7.3.2 Electrochemical Reaction Mechanisms

Most electrochemical reactions involve more than one simple charge transfer step. Prior to the charge transfer we find chemical reactions, equilibria as acid–base reactions, complexations or physical and chemical adsorption at the surface of the electrode. Often the products of the electrolysis are very reactive and they may further react chemically or electrochemically. The electrochemical product can even change the surface of the electrode, corroding the material or forming conducting or isolating layers on it. To gain insight into these processes in principle all the electrochemical methods discussed so far can contribute, but cyclovoltammetry has been established as the most powerful tool. Besides these pure electrochemical techniques, the combination of electrochemistry with other advanced techniques such as spectroscopy and microscopy and a careful analysis of the reaction products are advisable.

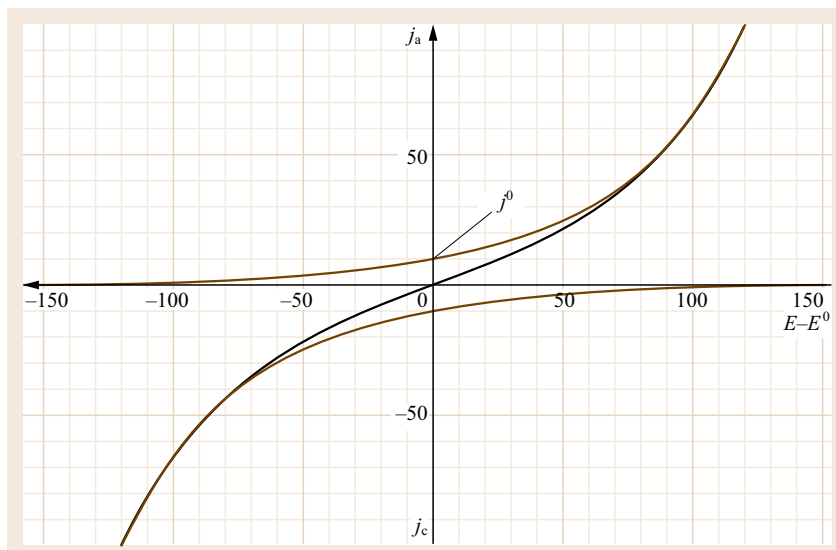


Fig. 7.35 Current density j (mA/cm^2) as a function of overvoltage $(E - E^0)$, $\alpha = 0.5k_c = 0.1 \text{ cm/s}$

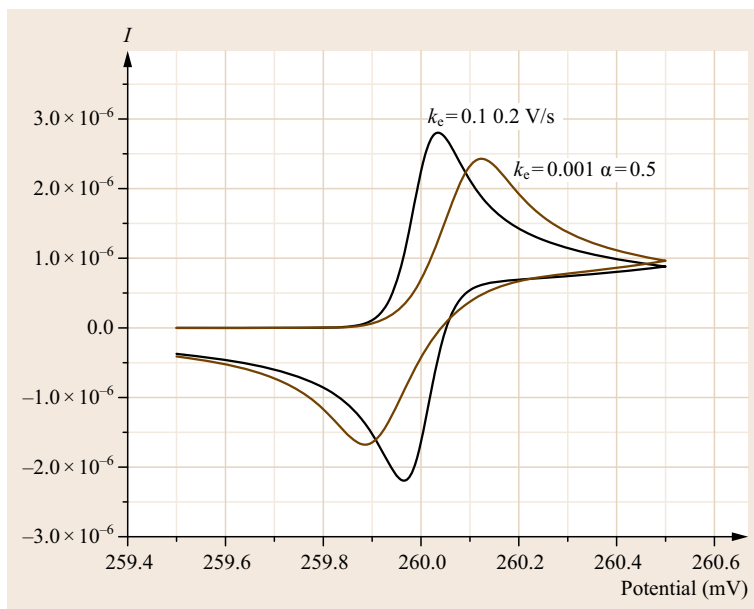


Fig. 7.36 CV with slow electron transfer heterogeneous rate constant 0.1 (*black*) and 0.001 cm/s (*brown*), scan rate 0.2 V/s

In the frame of this chapter a few examples shall be discussed:

1. After the first charge transfer further reversible peaks follow at higher potential. More than two subsequent reversible steps are seldom, because the concentration of high charge makes the molecule unstable and a quick irreversible decomposition follows. In C60 fullerene, however, even a six-step reversible reduction is possible: evidently this symmetric molecule enables a uniform distribution of the added electrons.
2. Slow reversible charge transfer. At slow scan rates the reaction rate remains diffusion-controlled, but at higher scan rates the current is limited due to the slow charge transfer. The peak current does not further increase with the square root of the scan rate and according to the Butler–Volmer equation an overvoltage is necessary to achieve a certain current. Thus, the difference between anodic and cathodic peak increases with the scan rate (Fig. 7.36).
3. The charge transfer is irreversible. No peak is found in the reverse part of the scan. Such reactions are of-

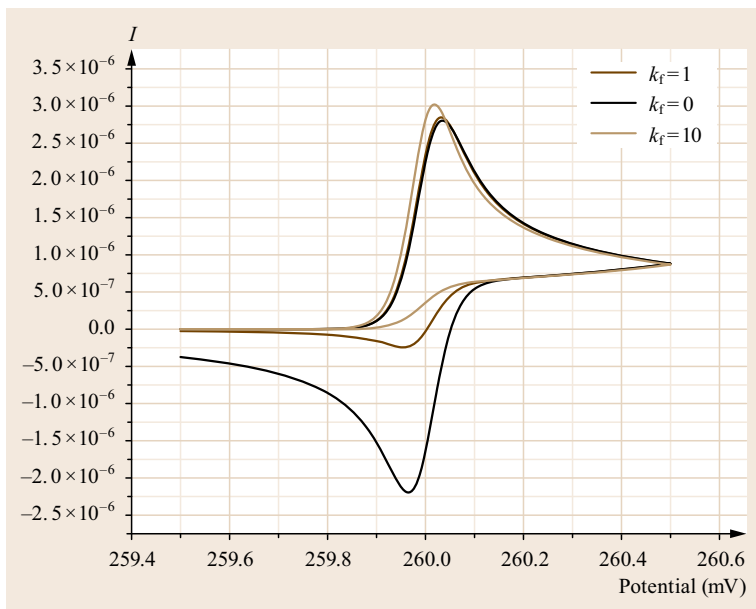


Fig. 7.37 EC mechanism, slow chemical reaction followed by charge transfer $k = 0.1 \text{ s}^{-1}$ (brown), quick reaction $k = 10 \text{ s}^{-1}$ (tan), no reaction (black) for comparison

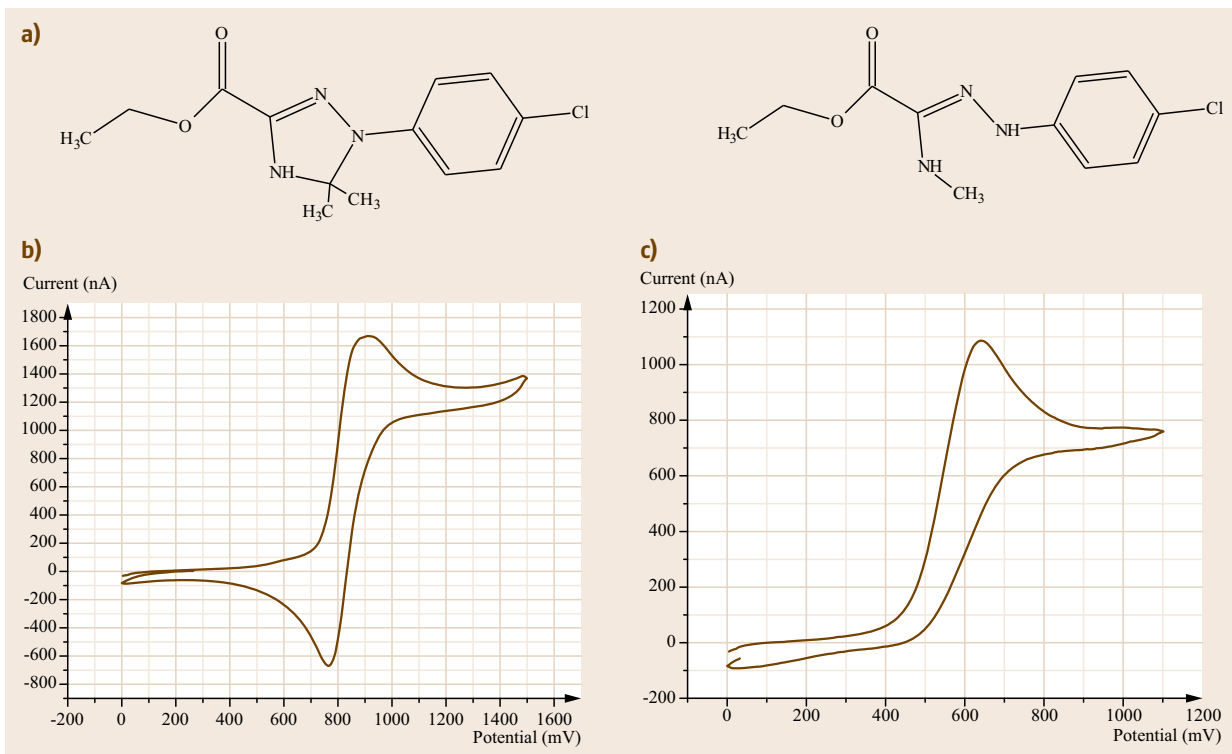


Fig. 7.38a–c Electrochemical oxidation of different amidrazone derivatives (a) Reversible oxidation (b) rapid decomposition of the primary oxidation product (c) presumably because of proton abstraction

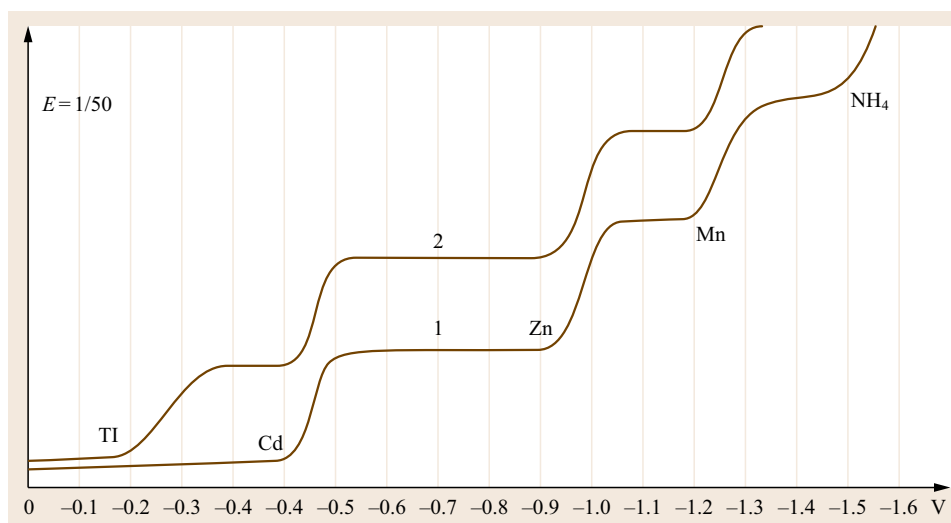


Fig. 7.39 Polarogram of a mixture of different cations. Concentrations 5×10^{-4} M, background electrolyte 0.01 M ammonia/ammonium chloride

- ten found when the charge transfer is accompanied by a fission of a bond.
- The charge transfer is followed by a chemical decomposition of the primary product, known as an EC mechanism. Depending on the reaction rate of the chemical reaction the reverse peak disappears as illustrated in Fig. 7.37. As an example, the oxidation of the triazoline derivative (a) yields a persistent radical cation that is reduced again during the reverse scan; the open-chained amidrazone (b) is readily decomposed after the oxidation.
 - The charge transfer is followed by a chemical reaction resulting in a product more electroactive than the educt. A second charge transfer follows at the same potential, known as an ECE mechanism. The electrochemical active substance is formed in an equilibrium step before the charge transfer (CE mechanism). The peak potential depends on the concentration of other components that are involved in the equilibrium.

The interpretation of CV data is a complex task and there exist several strategies, from correlations of peak currents and peak potential against scan rate to complete simulation of the whole diagram using digital simulation with finite elements. Often these programs are plugged into the instrument's software and allow for automatic parameter optimization to extract the kinetic and equilibrium constants. As an introduction to this field we recommend [7.24].

Amperometry with Convection at the Electrode

Convection strongly enhances the transport of all species from and to the electrode and limits the in-

fluence of diffusion to a thin layer immediately at the surface of the electrode. The concentration gradient through this layer comes in a constant steady state, depending on the velocity of the convection. In a single-sweep experiment we find a sigmoidal response function, independent of scan rate. Stirring or pumping the solution against the electrode as in HPLC-detectors or vibrating or rotating the electrode can realize a constant convection. In the case of a rotating disk electrode the limiting current is proportional to the square root of the speed of rotation (Levich equation)

$$j_L = 0.620zFD^{\frac{2}{3}}\omega^{\frac{1}{2}}\nu^{-\frac{1}{6}}c,$$

where j_L is the limiting current density, ω is the angular rotation rate of the electrode and ν is the kinematic viscosity.

The Levich equation is based on a pure diffusion-controlled charge transfer. Deviations can be attributed to a slow heterogeneous rate constant or other reactions linked with the charge transfer.

In polarography the moving boundary of the dropping mercury electrode causes a special form of convection. Together with the changing surface of the electrode, the mean current of this electrode is expressed by the Ilkovic equation. Figure 7.39 shows a typical polarogram.

Voltammetry with the dropping mercury electrode was introduced by Heyrovsky in the 1920s and was by far the most important electroanalytical technique for decades. The surface of the mercury electrode is ideally smooth and because it is renewed with every drop, it remains clean and even adsorption and desorption are reproducible. The high overvoltage of proton reduction enables very negative potentials in

protic solvents such as water. A wide range of anolytes, from metal cations, even alkali cations to organic compounds with nitro-, keto- or halogen are suitable for polarographic determination. Since the potential scan in polarography usually begins near zero and extends to the negative direction, the cathodic current

is plotted against the negative potential ($-E$ as abscissa).

During the almost hundred years of polarography a huge amount of literature has been published. For an introduction [7.25–29] may provide a non representative selection.

References

- 7.1 J. Koryta: Theory and application of ion-selective electrodes. Part 8, *Anal. Chim. Acta.* **223**, 1–30 (1990)
- 7.2 D.A. Skoog, D.M. West, F.J. Holler, S.R. Crouch: *Fundamentals of Analytical Chemistry* (Thomson Books Cole, New York 2004), Chap. 21
- 7.3 R. Buck: Electrochemistry of ion-selective electrodes, *Sens. Actuators* **1**, 197 (1981)
- 7.4 C.H. Hamann, A. Hamnett, W. Vielstich: *Electrochemistry* (Wiley-VCH, Weinheim 1998)
- 7.5 G. Eisenmann (Ed.): *Glass Electrodes for Hydrogen and Other Cations* (Marcel Dekker, New York 1967)
- 7.6 A. Michalska: All solid-state ion selective and all-solid-state reference electrodes, *Electroanalysis* **24**(6), 1223 (2012)
- 7.7 Sigma-Aldrich: Handbook Ionophores for ISE, <http://www.sigmaaldrich.com> (Sigma-Aldrich, St. Louis 2015)
- 7.8 W.E. Morf: *The Principles of Ion-Selective Electrodes and of Membrane Transport* (Elsevier, Amsterdam 1981)
- 7.9 E. Pretsch: The new wave of ion-selective, *Anal. Chem.* **74**(15), 420A–426A (2002)
- 7.10 Metrohm: Manual Ion selective Electrodes, 8.109.147612, <http://www.metrohm.com/en/products-overview> (Metrohm, Herisau 2016)
- 7.11 J. Bobacka, A. Ivaska, A. Lewenstam: Potentiometric ion sensors, *Chem. Rev.* **108**(14), 329–351 (2008)
- 7.12 T.R. Brumleve, R.P. Buck: Numerical solution of the Nernst-Planck and Poisson equation system with application to membrane electro-chemistry and solid state physics, *J. Electroanal. Chem.* **90**(1), 1–31 (1978)
- 7.13 T. Sokalski, P. Lingenfelter, A. Lewenstam: Numerical solution of the coupled Nernst-Planck and Poisson equations for liquid junction and ion-selective membrane potentials, *J. Phys. Chem.* **107**, 2443–2452 (2003)
- 7.14 T. Sokalski, T. Zwickl, E. Bakker, E. Pretsch: Lowering the detection limit of solvent polymeric ion-selective electrodes 1. Modeling the influence of steady-state ion fluxes, *Anal. Chem.* **71**, 1204–1209 (1999)
- 7.15 R.L. Solsky: Ion selective electrodes, *Anal. Chem.* **62**(12), 21R–33R (1990)
- 7.16 P. Lingenfelter, I. Bedlechowicz-Sliwakowska, T. Sokalski, M. Maj-Zurawska, A. Lewenstam: Time-dependent phenomena in the potential response of ion-selective electrodes treated by the Nernst-Planck and Poisson model-1. Intramembran process and selectivities, *Anal. Chem.* **78**, 6783–6791 (2006)
- 7.17 F.X. Rius-Ruiz, G.A. Crespo, D. Bejarano-Nosas, P. Blondeau, J. Riu: Potentiometric strip cell based on carbon nanotubes as transducer layer, *Anal. Chem.* **83**, 8810 (2011)
- 7.18 P. Bergveld: Development, operation, and application of ion-sensitive-field-effect-transistor as a tool for electrophysiology, *Biomed. Eng.* **19**(5), 342 (1972)
- 7.19 W. Moritz: Ionensensitive Feldeffekttransistoren-Beiträge zum Mechanismus der Potentialbildung und zur Optimierung der sensitiven Schicht, Dissertation (Humboldt Univ., Berlin 1985)
- 7.20 M. Mroczkirwicz, L. Gorski, A. Zamojska-Jaroszewicz, K.W. Szewczyk, E. Malinowska: Application of flow-injection potentiometric system for determination of total concentration of aliphatic carboxylic acids, *Talanta* **85**(4), 2047–2052 (2011)
- 7.21 J. Gallardo, S. Alegret, M. Del Valle: Application of potentiometric electronic tongue as a classification tool in food analysis, *Talanta* **66**(5), 1303–1309 (2005)
- 7.22 J. Tanyaniwa, S. Leuthardt, P.C. Hauser: Conductimetric and potentiometric detection in conventional and microchip capillary electrophoresis, *Electrophoresis* **23**, 3659 (2002)
- 7.23 V.Z. Karaoglanoff: Über Oxydations- und Reduktionsvorgänge bei Elektrolyse von Eisensalzlösungen, *Z. Elektrochem.* **12**(1) 5–16 (1906) in German
- 7.24 D.K. Gosser: *Cyclic Voltammetry* (Wiley, Weinheim 1993)
- 7.25 P. Bergveld: Thirty years of isfetology, what happened in the past 30 years and what may happen in the next 30 years, *Sens. Actuators B Chem.* **88**, 1–20 (2003)
- 7.26 J. Bobacka, A. Ivaska, A. Lewenstam: Potentiometric sensors, *Chem. Rev.* **108**, 329 (2008)
- 7.27 G. Henze: *Polarographie und Voltammetrie* (Springer, Berlin, Heidelberg 2001)
- 7.28 J. Wang: *Analytical Electrochemistry* 3 (Wiley-VCH, Weinheim 2006)
- 7.29 T. Riley, A. Watson: *Polarography and Other Voltammetric Methods* (Wiley, New York 1987)